Mapping cropping systems and their effects on ecosystem functioning and services in the Argentine Pampas

Pablo Baldassini[1-2-3*], Gonzalo Camba Sans[1-2], Domingo Alcaraz Segura[4-5], Cecilia Conde[2], José María Paruelo[1-2-3-6]

[1]LART, IFEVA, Universidad de Buenos Aires, CONICET, Facultad de Agronomía, Buenos Aires, Argentina.

[2]Departamento de Métodos Cuantitativos y Sistemas de Información, Facultad de Agronomía, Universidad de Buenos Aires, Argentina.

[3]Instituto Nacional de Investigaciones Agropecuarias. INIA La Estanzuela. Ruta 50 km 11. Colonia, Uruguay.

[4]Ecolab, Andalusian Inter-University Institute for Earth System Research (IISTA-CEAMA), Universidad de Granada, España.

[5]Departamento de Botánica, Facultad de Ciencias, Universidad de Granada, España.

[6]IECA. Facultad de Ciencias. Universidad de la República. Montevideo, Uruguay.

*pbaldass@agro.uba.ar (corresponding author)

Abstract

CONTEXT

The agricultural expansion and intensification modify the structure and functioning of ecosystems, which alter their capacity to provide ecosystem services (ES). An adequate analysis of these changes requires an exhaustive characterization of land use and land cover. In the Rio de La Plata Grassland (RPG), most of these characterizations are limited in terms of spatial or conceptual resolution since they generally differentiate coarse classes, such as winter and summer crops instead of crop types, at more than 30 meters.

OBJECTIVE

In this work, we propose to map crop types and cropping systems in one of the most productive agricultural areas of the RPG and assess their effects on ecosystem functioning and services.

METHODS

Preprint not peer reviewed

This preprint research paper has not been peer reviewed. Electronic copy available at: https://ssrn.com/abstract=4661637

Combine remote sensing data based on optical and microwave sensors provided by Sentinel 1 and 2 satellites (10 meters) to map crop types and cropping systems. Also, we used Landsat 8 images to characterize changes in albedo, Land Surface Temperature (LST) and evapotranspiration (ET) to analyze the environmental impacts of agriculture. Furthermore, we used Sentinel 2 to estimate the NDVI (a proxy of primary production) and the Ecosystem Services Supply Index (ESSI), a synoptic indicator that estimates provision and regulating ES related to water and carbon dynamics based on annual NDVI dynamics.

RESULTS AND CONCLUSIONS

We identified 14 crop types with an overall precision between 0.85 and 0.95. Winter crops were identified with a better precision than summer crops. Compared to native grasslands, the different cropping systems generated an increase in albedo and land surface temperature while evapotranspiration tended to be higher in systems that had more than one crop per year. The productivity (NDVI) and ecosystem services supply (ESSI) were the variables that showed the greatest variability. Schemes based on summer crops with cover crops and pastures would allow maintaining ecosystem functioning, which suggest the need to preserve and expand the area covered by production systems that keep the soil covered for much of the year.

SIGNIFICANCE

This work allowed us to evaluate the effect of cropping systems on ecosystem functioning and services supply, and provide information of interest for the future design, planning and implementation of sustainable productive development schemes.

Keywords: crop types classification, agriculture, ecosystem functioning, ecosystem services, remote sensing

1. Introduction

Global land use changes have occurred with unprecedented magnitude and intensity (Foley et al. 2005, Lambin and Meyfroidt 2011). These modifications represent one of the most crucial aspects of global change, given their profound impacts on various dimensions, such as the energy balance (Myhre and Myhre 2003, Schwaiger and Bird 2010), biodiversity loss (Pimm and Raven 2000, Newbold et al. 2015), the supply of Ecosystem Services (ES) (Rockström et al. 2009, Viglizzo et al. 2016), and climate change (Houghton et al. 2012). Temperate grasslands are among the most threatened

Preprint not peer reviewed

This preprint research paper has not been peer reviewed. Electronic copy available at: https://ssrn.com/abstract=4661637

biomes by human action (Hannah et al. 1995, Hoekstra et al. 2005). The Río de la Plata Grasslands (RPG), in Southern South America, represent one of the regions experiencing higher transformation rates (Paruelo et al. 2006, Jobbágy et al. 2006, Baldi and Paruelo 2008, Vega et al. 2009, Viglizzo et al. 2011, Modernel et al. 2016, Baeza and Paruelo, 2020, Paruelo et al. 2022). Since the 1990s, the diffusion of non-tillage systems and favorable economic and trade conditions promoted in the RPG the expansion and intensification of agricultural production (Viglizzo et al. 2001, Paruelo et al. 2005, Paruelo and Sierra, 2022) to unprecedented rates, resulting in the replacement of large extensions of grasslands with crops, pastures, and tree plantations (Paruelo et al. 2006, Baldi and Paruelo 2008, Baeza et al. 2014, Baeza and Paruelo 2020). These productive activities significantly modify the composition, structure and functioning of ecosystem, thereby altering their capacity to provide ecosystem services.

Ecosystem services (ES) are those aspects of ecosystems that are used (actively or passively) to produce human well-being (Fisher et al. 2009). Some "Intermediate services" which, in turn, determines the supply of final ES (Fisher et al 2009, de Groot et al. 2010) are associated to ecosystem functioning involves the exchange of matter (e.g., carbon and water) and energy (e.g., radiation and heat) between land surface, biota and the atmosphere (Virginia and Wall 2001, Lovett et al. 2006, Chapin et al. 2011). Most functional analysis focused on a particular functional process, the net primary production (NPP). NPP is an integrative descriptor of ecosystem functioning because it represents the total energy input (Tucker et al. 1985, Prince 1991, Lloyd 1990, Paruelo et al. 2001, Alcaraz-Segura et al. 2013). However, carbon gains dynamics by itself may not capture all aspects of ecosystem functioning (Regos et al. 2022, Marcos et al. 2022). Other dimensions need to be included for a comprehensive characterization of ecosystem functioning (Sun et al. 2008). Such dimensions include the energy balance (Nemani et al. 1997) and particularly some of its components: evapotranspiration (Kite and Pietroniro 1996) and albedo (Bala et al. 2007). Evapotranspiration is closely related to water regulation which, in turn, determines flood control (Bonan 2004, Campbell et al. 2007) or water supply. On the other hand, changes in terrestrial energy balance, such as the surface albedo, are associated with modifications in the regional climate (Pielke et al. 2011, Mahmood et al. 2014).

Two biophysical model capture the most critical aspect of ecosystem functioning: Monteith (1972) and the surface energy balance (Hall et al. 1992). Net primary production (NPP) is the rate at which vegetation fixes carbon, and it is proportional to the absorbed photosynthetically active radiation by vegetation (APAR) (Monteith 1972). The available energy represents the difference between global radiation and albedo, and it is primarily dissipated as sensible or latent heat flux, i.e., the evapotranspiration (composed of direct evaporation from the surface and vegetation-mediated transpiration). The albedo represents the shortwave radiation that is reflected by the earth's surface and can

This preprint research paper has not been peer reviewed. Electronic copy available at: https://ssrn.com/abstract=4661637

influence regional and global climate (Lawrence et al. 2022). Changes in surface albedo modify the radiation balance and the radiative forcing (RF) (Sieber et al. 2019), hence certain land use land changes (e.g., deforestation, afforestation or cover crop cultivation) could contribute to climate mitigation (Carrer et al. 2018, Lugato et al. 2020, Williams et al. 2021, Lawrence et al. 2022). The spectral information provided by satellites can be used to estimate these biophysical variables associated with ecosystem processes such as NPP (Ruimy et al. 1994), the surface energy balance (Hall et al. 1992) or evapotranspiration (Moran and Jackson 1991), using vegetation indices, albedo and land surface temperature (Jackson et al. 1977, Mu et al. 2007) (Figure 1). Specifically, the Normalized Difference Vegetation Index (NDVI, Tucker 1979) allows describing the spatial-temporal patterns of the NPP since they present a direct relationship with APAR (Potter et al. 1993; Ruimy et al. 1994; Los et al. al. 2000) and water losses due to evapotranspiration (Di Bella et al. 2000, Gallego et al. 2023).

Recently, the Ecosystem Services Supply Index (ESSI) was proposed like an integrative index of ecosystem functioning capable of describing the variation in different regulating and supporting ES (Paruelo et al. 2016). The ESSI is a synoptic indicator based on vegetation indices derived from remote sensing data, which constitutes a robust estimator of NPP, an integrating variable of ecosystem functioning (McNaughton et al., 1989). This index combines descriptors of amount and seasonality of the carbon captured by ecosystems through two attributes that can be estimated from the annual average of the NDVI (amount) and its intra-annual coefficient of variation (seasonality). This synoptic index explained an important proportion of the variability in the supply of several ES, such as soil carbon sequestration, underground and surface water regulation and bird species richness (Paruelo et al. 2016, Weyland et al. 2019, Jullian et al. 2021, Staiano et al 2021, Baldassini et al. 2023). The ESSI has been successfully applied in different biogeographical regions to assess the effects of land-cover change and degradation due to overgrazing on ecosystem functions and services (Milkovic et al. 2016, Verón et al. 2018, Altesor et al. 2019, Gallego et al. 2020, Camba Sans et al. 2021, Staiano et al. 2021, Paruelo et al. al. 2022). However, ESSI has not yet been used to analyze the influence that different agricultural management practices (i.e., cropping systems, rotations, etc.) may have on ecosystem services supply.

Due to its large spatial coverage and time frequency, remote sensing information has been frequently used to map land use/cover types (Paruelo 2008) at global (e.g. Friedl et al. 2010, Buchhorn et al. 2020, Brown et al. 2022), continental (e.g. Hugh et al. 2004, Giri and Long 2014), regional (e.g. Baeza et al. 2014, Baeza and Paruelo 2020, De Abelleyra et al. 2020, MapBiomas Pampa Project (https://.pampa.mapbiomas.org, Baeza et al. 2022)) and local scales (e.g., Guerschman et al. 2003, Baldi et al. 2008, De Abelleyra and Veron 2020). However, for the RPG region, most land use characterizations have been too coarse in terms of spatial and/or conceptual resolution

This preprint research paper has not been peer reviewed. Electronic copy available at: https://ssrn.com/abstract=4661637

Preprint not peer reviewed

since they only differentiated rough classes (such as winter and summer crops) but did not identify specific crop types. This has mainly been due to the use of a few multi-temporal data provided by a single sensor/satellite and/or due to a lack of detailed ground truth information to train classification algorithms. In recent years, the launch of new medium-high resolution optical and radar satellites, such as Sentinel-2A/B and Sentinel-1, respectively, has increased the availability of satellite images with higher spatial and temporal resolution (Vuolo et al. 2018, Segarra et al. 2020). Such ten meter-resolution data opens the possibility of characterizing the structural and functional aspects of terrestrial ecosystems and, hence, the differentiation of crop types (Kpienbaareh et al. 2021, Hu et al. 2021) with unprecedented detail. The combination of optical and microwave data improves the separability between different agricultural crops (Murthy et al. 2003, Deschamps et al. 2012, Foerster et al. 2012, Bargiel 2017), since optical data responds to the chemical properties of the vegetation while radar data is more related to vegetation structure and moisture (Haack et al. 2000).

The main goal of this work was to use high resolution satellite images to a) identify cropping systems in one of the most productive agricultural portions of the RPG, and b) evaluate the effects that different cropping systems have on ecosystem functions and services supply. For this, we first mapped the main 14 cropping systems by training random forests with Sentinel 1 and 2 data from ground surveys of 686 plots visited twice per year. Then, we compared the impact of these cropping systems on five biophysical variables that characterize the ecosystem functions and services derived from Landsat 8 and Sentinel 1 and 2 images: albedo, evapotranspiration (ET), Land Surface Temperature (LST), NDVI (a proxy of the primary production) and the Ecosystem Services Supply Index (ESSI).

2. Materials and methods

2.1. Study area

We focused our study on a transitional area among different subregions of the Río de la Plata Grassland region (RPG) (León 1991) that comprised the Rolling Pampa, Flat Inland Pampa and Flooding Pampa subregions (Figure 1). Cattle ranching was historically the main activity in the region, however, since the 90's agricultural expansion replaced large extensions of grasslands by crops and pastures (Viglizzo et al. 2001, Paruelo et al. 2007). Actually, agriculture is developed under no-till systems and without irrigation. Soybean and maize are the dominant summer crops and wheat is the dominant winter crop. Soybean and maize are mostly planted as a single crop (Waldner et al. 2016) during September–October (early soybean/maize) or in December–January (late maize) (De Abelleyra and Verón 2020). Wheat can be followed by soybean as a second crop (called

Preprint not peer reviewed
This preprint research paper has not been peer reviewed. Electronic copy available at: https://ssrn.com/abstract=4661637

second soybean) which result in a double cropping system (De Abelleyra and Verón 2020). Also, cover crops (usually called service crops) of 3–5 months can be included during fallow periods (Pinto et al. 2017), due to its positive effects on soil structure and fertility which benefit the subsequent commercial crops (Alvarez et al. 2017). Specifically, the study area was restricted to the Junin department (similar to county level), located in Buenos Aires province, Argentina (Figure 1), which covered and area close to 2,255 km^2. The average annual temperature is 18ºC and the annual mean rainfall is 1043 mm. The soil is, according to USDA Soil Taxonomy 2006 version, Junín series, coarse silt, mixed, thermic Typic Hapludoll (INTA, 2018). The area presents deep and dark soils suitable for agriculture with a predominant slope less than 1%.

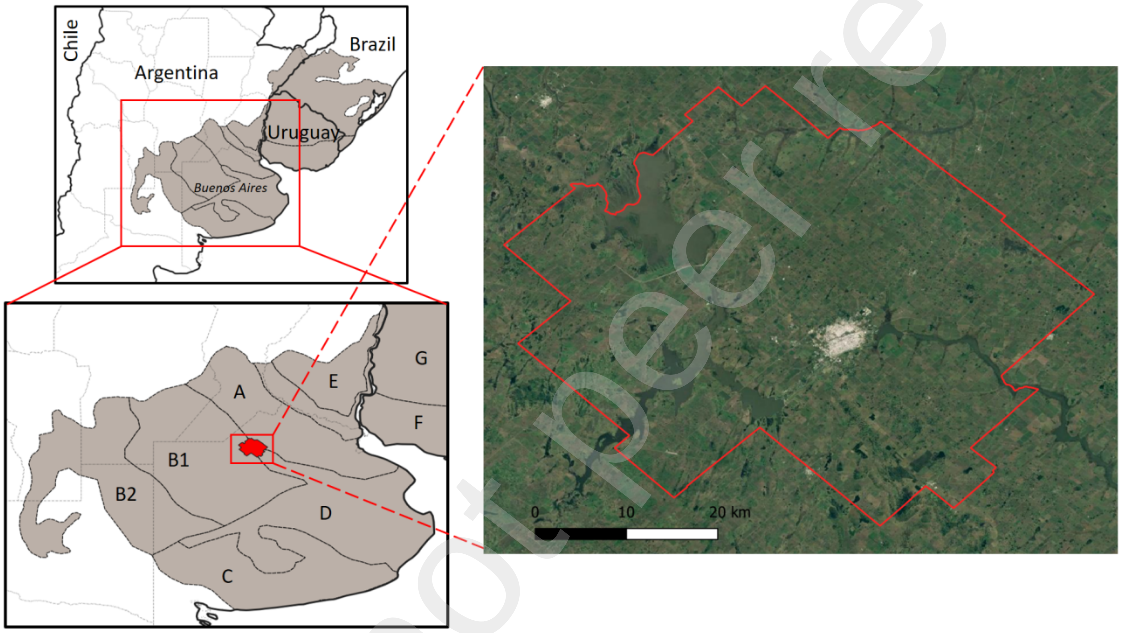

Figure 1. Study area corresponding to the department (or county) of Junín, province of Buenos Aires, Argentina. To the left the map shows the extension of the Río de la Plata Grassland region (RPG) (León, 1991), which is distributed in part of Argentina, Brazil and Uruguay. This region comprises different sub regions: (A) Rolling Pampa; (B1) Flat Inland Pampa; (B2) West Inland Pampa; (C) Southern Pampa; (D) Flooding Pampas; (E) Mesopotamian Pampas; (F) Southern Fields; (G) Northern Fields.

2.2. Field data

To characterize land cover at the crop type level, we used georeferenced surveys of crop information for the 2020-2021 growing season. These surveys were carried out in the field under the framework of Random Segments Method (Método de Segmentos Aleatorios, in Spanish) (MAGYP 2016) (Figure 2). This methodology consists of defining a series of random sampling segments on both sides of routes and roads, with a length

Preprint not peer reviewed

This preprint research paper has not been peer reviewed. Electronic copy available at: https://ssrn.com/abstract=4661637

close to 4 km and a width of 1 km (Figure 2). Therefore, the total area of each segment is approximately 400 ha. In the segments, productive land use of each plot is identified twice per growing season.

Land use data was available for a total of 686 plots identified along 28 random segments for two moments corresponding to the winter/spring season (where predominant crops were wheat, barley and oats) and the spring/summer season (where predominant crops were maize and soybean) (Figure 2). The average size of each plot was close to 13 ha and a negative buffer of 15 meters was made to discard plot edges. We defined 6 classes of crop type for the winter/spring season (wheat, barley, oats, fallow, pasture and grassland), and 8 classes of crop type for the spring/summer season (early maize, late maize, soybean, second soybean, fallow, pasture, grassland and other summer crops) based on ground surveys information.

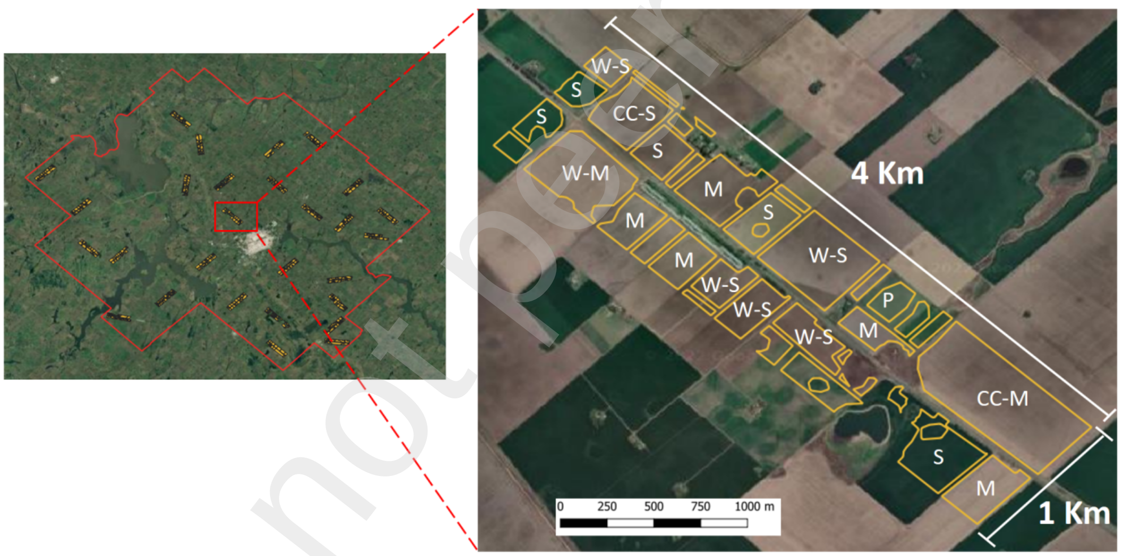

Figure 2. Illustration of the field data at crop type level for the Junín department surveyed under the framework of Random Segments Method (MAGYP 2016). Productive land uses were identified in 686 plots along 28 random segments. Each segment has a length close to 4 km and a width of 1 km. Plots averaged 13 ha. Land use data was surveyed for two moments, the winter/spring season and the spring/summer season. The letters indicate the crop types (S: soybean, M: Maize, W: Wheat, CC: Cover Crop, P: Pasture).

2.3. Images processing and classification of crop types and cropping systems

We used images from Sentinel-1 radar and Sentinel-2A/B surface reflectance (SR) from 2020-06-01 to 2021-05-31. Sentinel-1 images have a spatial resolution of 10 meters and a revisit period of 12 days. Also, they have the advantage that radar signal is not

Preprint not peer reviewed

This preprint research paper has not been peer reviewed. Electronic copy available at: https://ssrn.com/abstract=4661637

affected by clouds. We used the Sentinel-1 Ground Range Detected (GRD) scenes which images are pre-processed applying thermal noise removal, radiometric calibration and terrain correction. A mono-temporal speckle filter was applied using a smoothing radius of 50 meters to smooth images and reduce noise (Copernicus Sentinel data 2023). The data selected corresponded to single co-polarization and dual cross-polarization bands (i.e., “VV” and “VH”). The “VH” (or “HV”) is the most important to identify most crops (Brisco et al. 1992, Lee et al. 2001) due to its responsiveness to multiple scattering from the vegetation volume (Valcarce-Diñeiro et al. 2019). However, a significant improvement in accuracy was observed when adding a polarimetric channel, being the “VV” the second better polarization (Foody et al. 1994).

The Sentinel-2 images have a spatial resolution of 10 meters and 20 meters (depending on the band) and a temporal resolution of 3-5 days. We used the Sentinel-2 Level 2-A surface reflectance images. Clouds were masked by using the S2 cloud probability dataset (s2cloudless) and shadows by using the cloud projection intersection with low-reflectance near-infrared (NIR) pixels. For each image, we selected the bands B2 (blue), B3 (green), B4 (red), B8 (NIR), B11 (SWIR1) and B12 (SWIR2) and to calculate four normalize difference spectral indices: NDVI (Normalized Difference Vegetation Index), GNDVI (Green Normalized Difference Vegetation Index), NDMI (Normalized Difference Moisture Index) and NBRI (Normalized Burn Ratio Index) (Appendix). NDVI is highly associated with vegetation cover (Running 1990), GNDVI is a modified version of NDVI to be more sensitive to the variation of vegetation chlorophyll content (Gitelson et al. 1996), NDMI is used to determine vegetation water content (Hardinsky et al. 1983) and NBRI is sensitive to vegetation changes (Key and Benson 1999). For Sentinel-1 and Sentinel-2, we reduced the data to 2-month intervals by obtaining the median value for each band and index. Also, for Sentinel-2, we calculated statistics metrics for each band for the whole period that summarize the phenological behavior of the vegetation (i.e., mean, minimum, maximum, Julian date of maximum and standard deviation).

Field data from the Random Segments Method was used to train a Random Forest supervised classification algorithm and to evaluate the classifications. Random Forest consists of an ensemble of classification trees, in which each tree is randomly generated and individually trained to finally select the most accurate classifier, and it is one of the most successfully used in remote sensing (Li et al. 2016, Teluguntla et al. 2018, Maxwell et al. 2019). This method was applied with 150 trees and performed at the pixel level. A total of 7500 pixels were randomly and stratified sampled, considering the proportion of each class in the field data. Around 70% of pixels (close to 5,000 pixels) were used for training the classification algorithm and the remaining 30% (close to 2,500 pixels) were used for evaluation. We generated two classifications, one for winter/spring growing season (June 1st to December 31st) and another for spring/summer growing season (September 1st to May 31st of the next year), including 97 and 110 data bands

Preprint not peer reviewed
This preprint research paper has not been peer reviewed. Electronic copy available at: https://ssrn.com/abstract=4661637

respectively. A median filter with a window of 3x3 pixels was applied over each classification to minimize the salt and pepper effects (Chuvieco, 1990).

We evaluated the performance of each classification by calculating the overall accuracy, the user's and producer's accuracy and the F1-score. The F1-score is an integral index that combines the user´s accuracy (precision) and the producer's accuracy (recall) for each class as follows: *2 * (precision * recall) / (precision + recall)*. The global F1-score or mean value across all classes can be interpreted as the overall accuracy. Once cropland maps for each season were generated, a pixel-based annual crop sequence was defined as the sum of both classifications, identifying a total of 12 cropping systems in addition to grassland: wheat-maize, wheat-soybean, pasture, barley-maize, barley-soybean, oat-maize, oat-soybean, early maize, late maize, soybean, cover crop-maize and cover crop-soybean. Cover crops corresponded to situations where pastures were identified in winter/spring season followed by a summer crop in spring/summer season. In the same way, pastures were considered in those situations where a winter crop was identified in winter/spring season followed by a pasture in spring/summer season. Winter forage crops are annual pastures based on wheat, oat or barley among others (Kent 2019) and they are often confused with winter crops. In turn, a class called *Other classes* was incorporated that included other summer crops different to maize and soybean and unlikely situations, probably associated with classification errors. A mask of water bodies, rivers, urban areas and woody covers was applied based on JRC Yearly Water Classification History v1.3 product (Pekel et al. 2016), GIS layer from Argentine National Geographic Institute (IGN - URL: http://www.ign.gob.ar/NuestrasActividades/InformacionGeospatial/CapasSIG) and MapBiomas Pampa project (https://.pampa.mapbiomas.org, Baeza et al. 2022).

All processes were performed using Google Earth Engine (Gorelick et al. 2017) and QGIS 3.4 Madeira (QGIS 2019). The Google Earth Engine cloud platform allow processing large volumes of geospatial data, improving geospatial processing and analysis capacity.

2.4. Images processing to derive biophysical variables

Biophysical variables related to water dynamics and energy balance (i.e., albedo, Land Surface Temperature (LST) and evapotranspiration (ET)) were derived from Landsat 8, while those related to carbon gains dynamics and ESSI were derived from Sentinel-2. A total of 28 Landsat 8 OLI/TIRS images were used (scenes 227/84 and 226/84) that cover the study area. Selected images encompassed the growing season and were distributed between July 2020 and June 2021. Images were downloaded from Google Earth Engine (GEE) platform (Gorelick et al. 2017) and they corresponded to

This preprint research paper has not been peer reviewed. Electronic copy available at: https://ssrn.com/abstract=4661637
Preprint not peer reviewed

Collection 2 Tier 1 level 2 for atmospherically corrected surface reflectance and land surface temperature bands. The images were previously filtered by quality, discarding the pixels that presented clouds and shadows by using the *QA_PIXEL* band. The images were processed in R using the *rgdal, raster* and *sp* packages. Subsequently, the processed images were uploaded back to GEE. For each pixel, we first calculated the median of each variable per month and then the mean and the coefficient of variation (cv) along the growing season by cropping system.

For albedo, we applied the algorithm proposed by Liang (2000):

$$\alpha = 0.356\ \lambda B2 + 0.130\ \lambda B4 + 0.373\ \lambda B5 + 0.085\ \lambda B6 + 0.072\ \lambda B7 - 0.0018$$

where each of the coefficients represents the proportion in which each band contributes to the estimation of albedo. λB2, λB4, λB5, λB6 and λB7 correspond to the reflectance bands of the portions of blue (0.452-0.512 μm), red (0.636-0.673 μm), near infrared (0.851-0.879 μm), shortwave infrared 1 (1.566 -1,651 μm) and shortwave infrared 2 (2,107-2,294 μm), respectively.

For Land Surface Temperature (LST), we used the *B10 surface temperature* band and applyed the following “mono-window” correction algorithm proposed by Qin et al. (2001):

$$LST\ (°K) = (h^*(1-C-D)+(k^*(1-C-D)+C+D)^*B10-(D^*Tef))/C$$

where h= -63.1885 and k= 0.44411 are constants related to the temperature range of the area according to Qin et al. (2001), Tef is the mean effective atmospheric temperature, *C* and *D* are coefficients defined as: (c) C = ε x t (d) D = (1- t) [1+ (1- ε) t] where, *ε* represents the emissivity that can be estimated from the Normalized Difference Vegetation Index (NDVI) according to the methodology proposed by Van de Griend and Owe (1993) and *t* is the atmospheric transmittance (g cm^{-2}) estimated from the moisture content according to Qin et al. (2001).

For actual daily evapotranspiration (ET), we used the simplified energy balance method proposed by Jackson (1985), which estimates ET from Land Surface Temperature (LST) and net radiation based as follows:

$$ET = Rn - B\ (Ts - Ta)^{n}$$

where *Rn* is the net radiation (Mj m^{-2}), *Ts* is the Land Surface Temperature (°K), *Ta* is the average air temperature (°K) and *B* and *n* are semi-empirical parameters that vary according to the vegetation type. The net radiation was estimated as the balance between the net incident shortwave radiation *Sn* (Mj m^{-2} day^{-1}) (Appendix) and the net emitted longwave radiation *Ln* (Mj m^{-2} day^{-1}) as proposed by Granger (2000) (Appendix). The differential temperature *Ts-Ta* was estimated from the corrected surface temperature *Ts*.

Preprint not peer reviewed

This preprint research paper has not been peer reviewed. Electronic copy available at: https://ssrn.com/abstract=4661637

The air temperature *Ta* were derived from the Junín Aero meteorological station (34° 33′ S, 61° 00′ W) belonging to the Argentinean National Meteorological Service (SMN). The sinusoidal behavior of temperature was considered to estimate *Ta* at the time of image acquisition. Ta = Tmean+[(Tmax – Tmin)/2] sin 360[(20 – h)/24] where *Tmean, Tmax* and *Tmin* are daily temperature data (°C), and *h* is the hour at which it is needed to estimate the temperature (2:00 p.m. for the Landsat satellite). To obtain the parameters *B* and *n*, the NDVI was first calculated as the ratio between the reflectance of the near-infrared (NIR) and red (R) bands from Landsat: NDVI = (NIR–R/NIR+R). Then, the 1st and 99th percentile was calculated for all dates and the maximum (0.92) and minimum (0.2167) values were identified to scale the index, as suggested by Carlson et al. (1995). From this new scaled index (NDVI* = ($NDVI-NDVI_{MIN}$)/($NDVI_{MAX}-NDVI_{MIN}$)), the coefficients *B* and *n* were estimated (B=0.0109+(0.051*NDVI*), n=1.067–(0.372*NDVI*)). The coefficient *B* reflects the integrated daily average of the sensible heat conductance in the vegetation that depends on the roughness and the speed of the wind. The coefficient *n* represents a correction for non-neutral static stability conditions that generally assumes values close to 1. This approach has been used satisfactorily in different environments and with different plant covers (crops, grasslands, and forests; Caselles et al. 1998; Nosetto et al., 2005, Milkovic et al. 2019).

The average NDVI from the whole growing season, derived from Sentinel-2 images were used as a proxy of carbon gains or net primary production (NPP). This index has shown a strong relationship with the fraction of photosynthetically active radiation intercepted by green tissues and thus with the ANPP (Huete et al. 2002, Paruelo 2008). In turn, we calculated the coefficient of variation along the growing season to compute the Ecosystem Services Supply Index (ESSI) (Paruelo et al. 2016, Staiano et al. 2021). This index is calculated as ESSI = NDVImean*(1–NDVIcv) and ranges from 0 to 1, where the sites that present higher values are those that supply more ecosystem services associated with the dynamics of water and carbon. We applied a mask to the Sentinel-2 images to discard pixels with clouds and cloud shadows (as explained in section 2.4). We reduced the data to monthly median values to avoid imbalance in descriptive statistic calculations due to missing values. From these 12 composites we calculated the *NDVImean* and the *NDVIcv*.

To assess the effects on ecosystem functions and services supply, we calculated the differences for each cropping system compared to natural grasslands, the pristine land cover in the study area. For this, we extracted the average values, the standard deviation of the annual mean and the coefficient of variation along the growing season for LST, albedo, ET, NDVI and ESSI for each cropping system. We calculated the average relative effect of land transformation on each biophysical variable, i.e., the change from grassland to another cropping system. Thus, we obtained the relative effect of land use changes in terms of matter, energy and water exchanges. Because all the pixels of each

This preprint research paper has not been peer reviewed. Electronic copy available at: https://ssrn.com/abstract=4661637

class identified by the image classifications were considered (i.e., the data correspond to all the observational units, that is, it is a census, not a sampling), we did not perform statistical tests to analyze whether the differences between cropping systems with respect to grassland were statistically significant. On the other hands, we also tested the relationship between the biophysical variables with a Pearson correlation analysis considering a $\alpha=0.05$.

3. Results

3.1. Crop type and cropping system mapping

Crop type classifications showed high overall accuracy (global F1-score), with better average performance for the winter/spring classification than for the spring/summer classification (0.946 vs 0.846, Figure 3 and Table 1). The user's accuracy, the producer's accuracy and the F1-score were also high, with values between 0.8 and 0.9 for spring/summer and between 0.9 and 0.97 for winter/spring classification (Table 1). Winter crops (wheat, barley, oat) and fallow classes showed higher precision than pasture and grassland (Figure 3 and Table 1). These classes showed a better performance than summer crops, within which soybean showed the lowest F1 (Table 1). In terms of percentage covered in the study area, within the winter crops, wheat was the most abundant (16%), while barley and oat occupied less than 3% (Table 1). Winter/spring fallow occupied the highest proportion of the study area (38.7%), overpassing the area of pastures and grasslands (Table 1). Among summer crops, soybean occupied most of the study area (over 40%), followed by maize (14%). Most of the maize was early sown (Figure 3 and Table 1). Double cropping systems other than wheat-soybean, and cover crops occupied around 4% of the area (Figure 4 and Table 1). The class *Other classes* that included other summer crops different to maize and soybean and unlikely situations showed a low area cover (2.6% of the study area) (Figure 4 and Table 1).

Preprint not peer reviewed

This preprint research paper has not been peer reviewed. Electronic copy available at: https://ssrn.com/abstract=4661637

winter/spring classification

Winter crop types	User accuracy	Producer accuracy	F1-score	Area proportion
Wheat	0.96	0.98	0.97	0.16
Barley	1	0.96	0.98	0.007
Oat	0.96	0.92	0.94	0.0276
Fallow	0.97	0.96	0.97	0.387
Pasture	0.90	0.92	0.91	0.061
Grassland	0.87	0.91	0.89	0.222
Mask	-	-		0.132

spring/summer classification

Summer crop types	User accuracy	Producer accuracy	F1-score	Area proportion
Early maize	0.85	0.79	0.82	0.142
Late maize	0.97	0.83	0.90	0.012
Soybean	0.76	0.87	0.81	0.257
Fallow	0.93	0.82	0.87	0.02
Pasture	0.84	0.83	0.84	0.057
Grassland	0.85	0.96	0.90	0.2
Other summer crops	0.93	0.87	0.90	0.0158
Second soybean	0.87	0.84	0.85	0.161
Mask	-	-	-	0.132

annual classification or cropping systems

Cropping systems	Area proportion
Wheat-maize	0.009
Wheat-soybean	0.145
Pasture	0.080
Barely-Maize	0.000
Barley-soybean	0.007
Oat-maize	0.004
Oat-soybean	0.016
Early maize	0.139
Late maize	0.002
Soybean	0.246
CC-maize	0.001
CC-soybean	0.005
Grassland	0.185
Other classes	0.026
Mask	0.133

Table 1. User accuracy, producer accuracy, F1-score and area proportion for crop type to each classification. The winter/spring classification showed an overall accuracy (global F1-score) of 0.946, while the spring/summer classification showed an overall accuracy of 0.846. The annual classification or cropping systems only shows the area proportion for each class due to it was not possible evaluate the precision.

Preprint not peer reviewed

This preprint research paper has not been peer reviewed. Electronic copy available at: https://ssrn.com/abstract=4661637

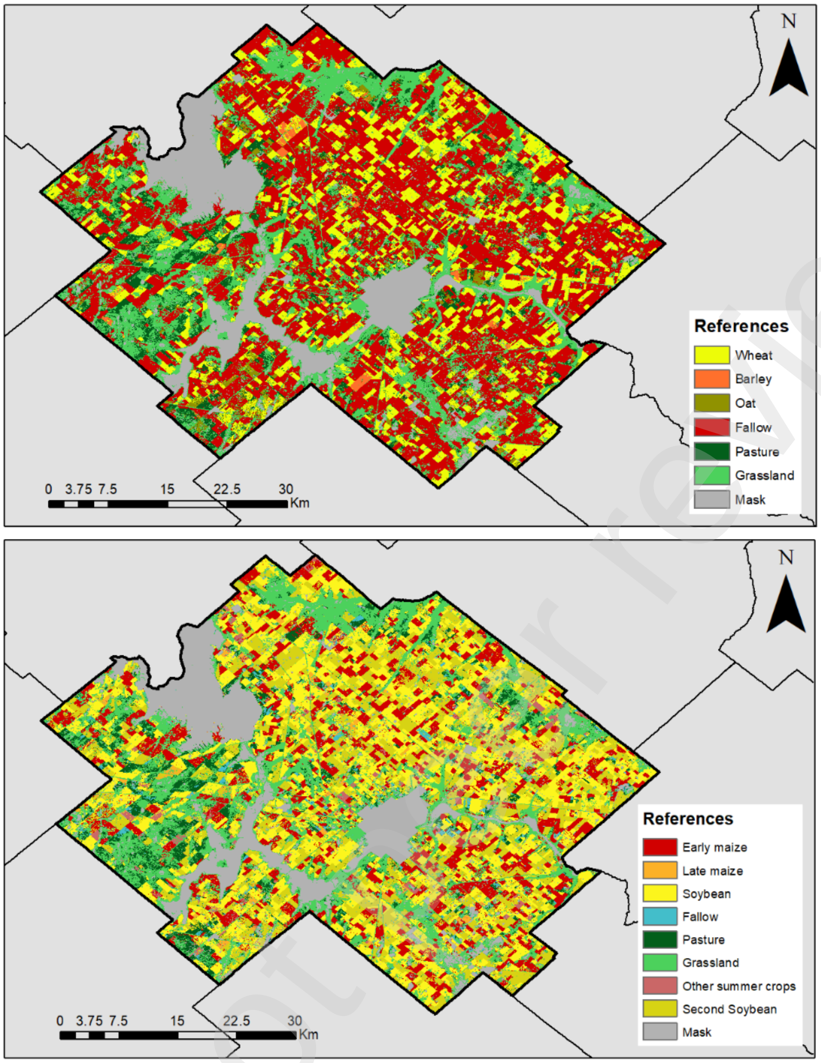

Figure 3. Supervised classifications of crop types for winter/spring season (top) and spring/summer season (bottom). We combined data from Sentinel 1 and Sentinel 2A/B satellites and used the Random Forest algorithm. For the winter/spring classification, 6 classes were identified: Wheat, Barley, Oat, Fallow, Pasture and Grassland, while for the spring/summer classification 8 classes were identified: Early maize, Late Maize, Soybean, Fallow, Pasture, Grassland, Other summer crops and Second soybean. Also, the water bodies, rivers, urban areas and woody covers were masked using auxiliary information.

Preprint not peer reviewed

This preprint research paper has not been peer reviewed. Electronic copy available at: https://ssrn.com/abstract=4661637

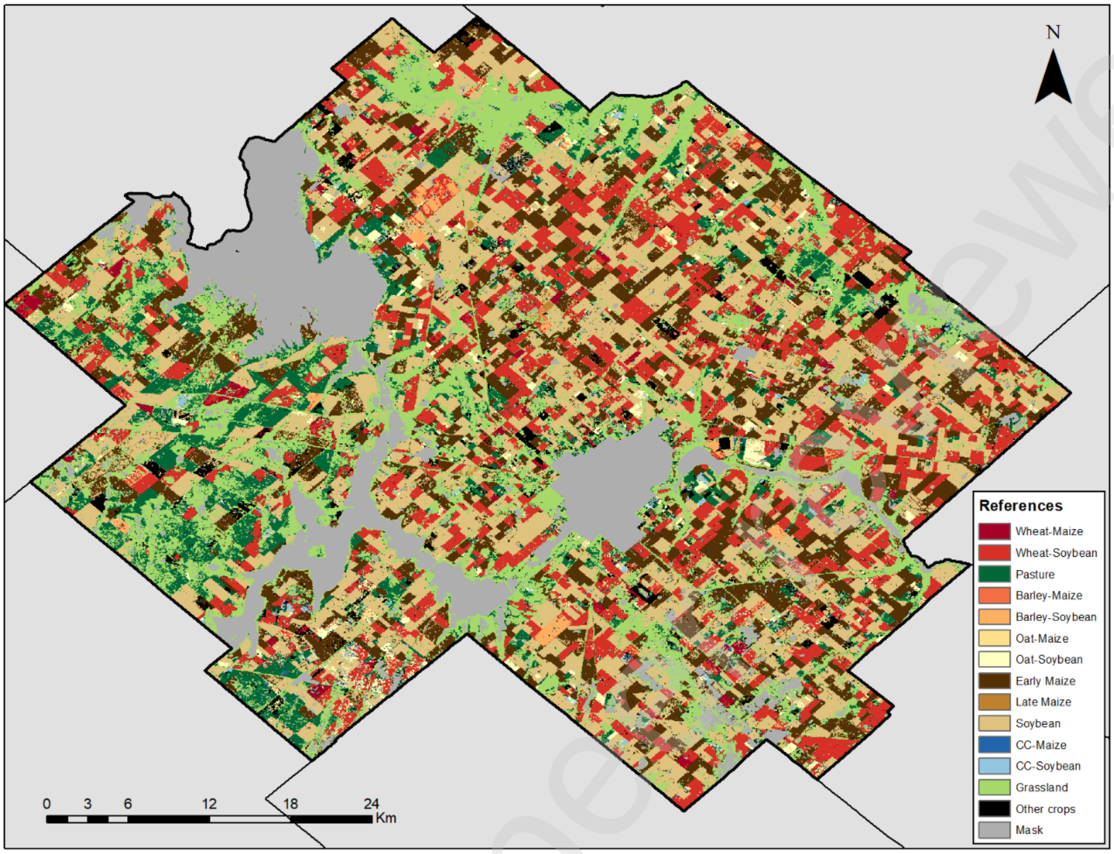

Figure 4. Cropping systems obtained from the combination of the winter/spring season and spring/summer season classifications. A total of 12 cropping systems were identified in addition to natural grasslands: wheat-maize, wheat-soybean, pasture, barley-maize, barley-soybean, oat-maize, oat-soybean, early maize, late Maize, soybean, cover crop (CC)-maize and cover crop (CC)-soybean. We included a class called *Other crops* that included other summer crops different to maize and soybean and unlikely situations occurrences, probably associated with errors in the classification process. Also, the water bodies, rivers, urban areas and woody covers were masked using auxiliary information.

3.2. Biophysical effects of cropping systems compared to grasslands

Cropping systems did not differ much from grasslands in Land Surface Temperature (LST), albedo and average daily evapotranspiration, but greater differences were observed in the NDVI and in the Ecosystem Service Supply Index (ESSI) (Figures 5, 6 and 7). The average albedo was 0.149 for grasslands and it ranged from 0.152 to 0.174 for the different cropping systems, representing an average increase between 1.64 and 16.35% (Figures 5 and 7). No association was observed between albedo changes and cropping system (i.e., double cropping, single summer crops, summer crops with cover crop), however, soybean always showed a higher albedo than maize. Thus, the presence of soybean increased the albedo, on average, by 3.92, 4.24, and 8.5% under summer crops with cover crop, double cropping and single summer crops, respectively

Preprint not peer reviewed

This preprint research paper has not been peer reviewed. Electronic copy available at: https://ssrn.com/abstract=4661637

compared to maize (Figures 6 and 7). In addition, single soybean crops showed one of the highest albedo values (17%, i.e., a 14.39% higher than grasslands), being surpassed only by pastures. The pastures showed the highest albedo values, being 0.179, that is, 16.35% higher than grasslands (Figures 5 and 7).

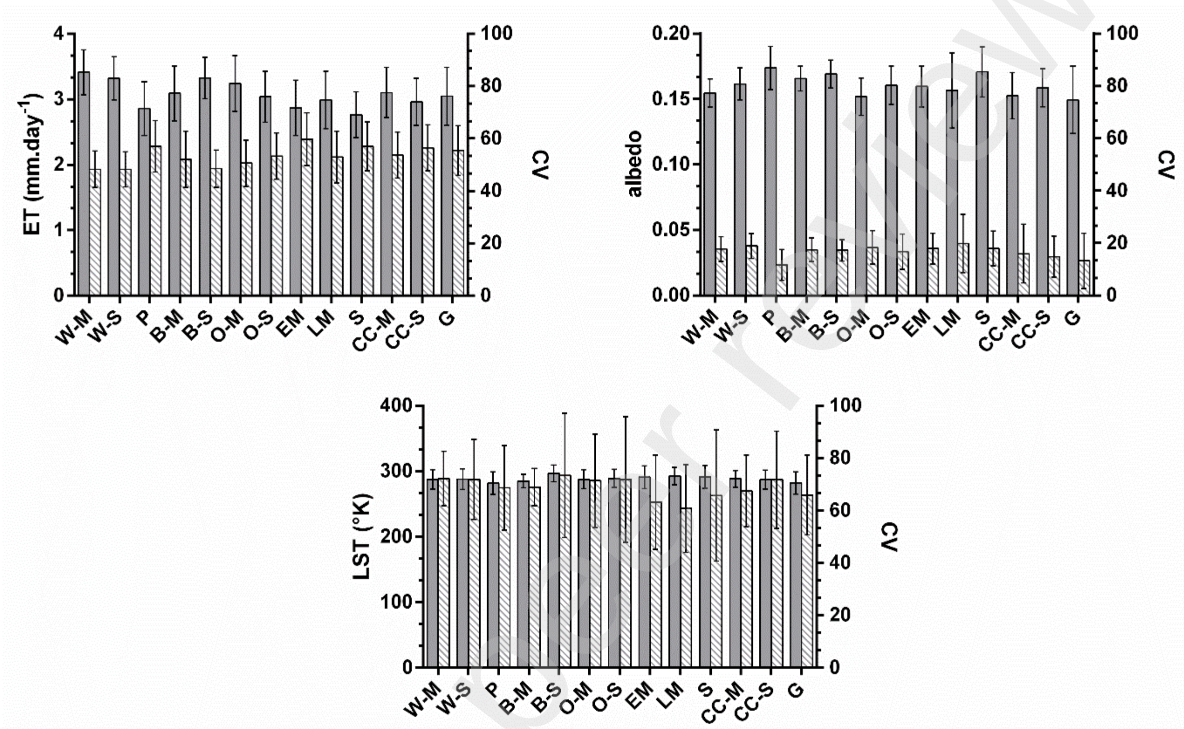

Figure 5. Functional vegetation attributes based on Landsat images calculated for each cropping system identified at annual classification: evapotranspiration (ET in mm/day), albedo and Land Surface Temperature (LST in °K). The columns indicate the average values while the lines indicate the standard deviation.

Regarding evapotranspiration, the double cropping was the only system that showed higher values compared to grassland, being up to 12.05% greater (3.41 mm/day vs 3.04 mm/day) (Figures 5 and 7). On the contrary, pastures and single summer crops showed values between 1.78 and 9.24% lower than grasslands, having soybean the lowest value (2.76 mm/day). Summer crops with cover crops showed very similar values, although those with maize showed slightly higher values and those with soybeans showed slightly lower values (Figures 5 and 7). At the same time, the cropping systems that showed higher ET mean were those that, in turn, showed a less seasonal variation ($r=-0.93$, p-value < 0.0001) (Figures 5 and 7 and Table 2). Land Surface Temperature (LST) varied little in a relative way but a lot in an absolute way. Thus, the maximum variations were around 5% with respect to the grassland, but they represented changes up to 14.47 °K (Figures 5 and 7). Pastures practically did not differ from the grasslands

Preprint not peer reviewed

This preprint research paper has not been peer reviewed. Electronic copy available at: https://ssrn.com/abstract=4661637

(282.045 °K vs 282.401 °K), while the single summer crops showed higher values than the double cropping and summer crops with cover crop (291.88 °K vs 289.16 °K and 287.24 °K) (Figures 5 and 7).

	ET	LST	albedo	ETcv	LSTcv	albedocv	NDVImean	ESSI	NDVIcv
ET	1	0.64	0.26	<0.001	0.02	0.28	0.06	0.66	0.27
LST	0.14	1	0.58	0.44	0.89	0.01	0.05	0.0023	0.01
albedo	-0.34	0.17	1	0.63	0.7	0.66	0.71	0.53	0.33
ETcv	-0.93	-0.23	0.15	1	0.03	0.13	0.11	0.97	0.52
LSTcv	0.64	-0.04	0.12	-0.6	1	0.72	0.01	0.23	0.15
albedocv	0.33	0.68	-0.14	-0.44	-0.11	1	0.18	<0.001	0.01
NDVImean	0.53	-0.55	-0.11	-0.47	0.68	-0.39	1	0.0013	<0.001
ESSI	0.13	-0.77	-0.19	0.01	0.35	-0.82	0.79	1	<0.001
NDVIcv	-0.33	0.67	0.3	0.2	-0.43	0.67	-0.87	-0.96	1

Table 2. Correlation between the biophysical variables calculated for each cropping system. Values below the diagonal indicate the Pearson correlation index (which varies between -1 and 1 for negative and positive correlations, respectively), while values above the diagonal indicate the p-value (α=0.05)). The red colors indicate negative values while the blue ones positive values, while the intensity of the color indicates the magnitude of the relationship. White and light colors indicate absence of correlation.

The seasonal variation in the biophysical variables analyzed was greater for the Land Surface Temperature (LST), followed by evapotranspiration and albedo, being an average of 68%, 53% and 17%, respectively (Figures 5 and 7). However, the relative changes between the different cropping systems compared to grassland showed the inverse pattern, being higher for albedo, followed by evapotranspiration and LST (Figures 5 and 7). Thus, seasonality of albedo increased compared to grassland between 12 and 50%, being higher for single summer crops, intermediate for double cropping and lower for summer crops with cover crops (Figures 5 and 7). Pastures, on the contrary, reduced the seasonal variation around 11% (Figures 5 and 7). In the case of ET, the seasonal variation decreased between 3.1 and 13% under more diverse cropping systems (i.e., double cropping and summer crops with cover crops), while it increased between 2.8 and 7.75% in pastures and single summer crops (Figures 5 and 7). The seasonal variation of the LST increased between 2.5 and 11.5% in double cropping, pastures and summer crops with cover crops, while it showed a reduction between 0.1 and 7.65% in single summer crops (Figures 5 and 7).

Double cropping, summer crops with cover crops and pastures showed higher productivity, with higher average NDVI values in comparison to grassland (which had 0.54, 0.55, 0.58 and 0.49, respectively) (Figures 6 and 7). These increases ranged from 1% to 21%, observing average NDVI values of up to 0.6 (barley-maize) (Figures 6 and 7). On the other hand, single summer crops showed lower productivity (NDVI were 0.33, 0.37 and 0.39 for soybean, early maize and late maize, respectively) with decreases

Preprint not peer reviewed

This preprint research paper has not been peer reviewed. Electronic copy available at: https://ssrn.com/abstract=4661637

between 20 and 31% in comparison to grassland (Figures 6 and 7). Likewise, the less productive crop types tended to show a greater seasonality in productivity (r=-0.87, p-value<0.0001) (Figures 6 and 7 and Table 2). Thus, single summer crops showed an increase in the seasonal variation between 130 and 223% compared to grassland, while for double cropping the increase was between 39 and 87%. Pastures, on the other hand, reduced seasonality of productivity by around 22% (Figures 6 and 7).

All crop types showed lower ESSI values compared to grassland (0.718), except for pastures (Figures 6 and 7). These decreases were, on average, 11% and 22% for double cropping and single summer crops, respectively, whose ESSI values were 0.64 and 0.55 (Figures 6 and 7). Summer crops with cover crops, on the other hand, showed a slight decrease of around 2.5% in comparison to grassland, showing average ESSI values of 0.7. Finally, pastures showed a slight increase in the ESSI of around 5% (0.76) compared to grassland (Figures 6 and 7). The variation of the ESSI along cropping systems was more associated with the seasonal variation of the NDVI (NDVIcv) (r=-0.96, p-value<0.0001) (Figures 6 and 7 and Table 2) than with changes in the NDVI mean (NDVImean) (r= 0.85, p-value<0.0001) (Figures 6 and 7 and Table 2).

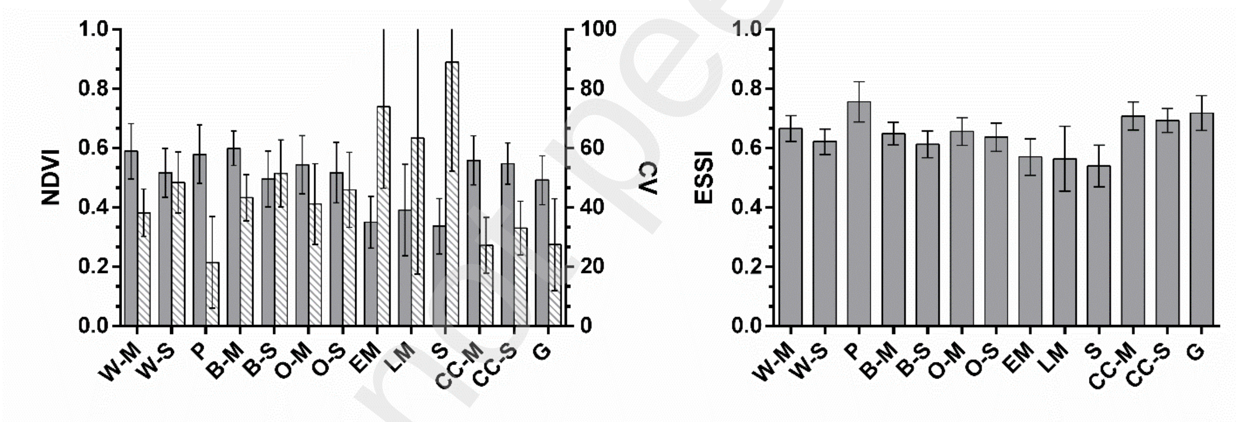

Figure 6. NDVI (as a proxy for aboveground net primary productivity) and ESSI (Ecosystem Services Supply Index) values calculated from data provided by the Sentinel 2 for each cropping system identified at annual classification. The columns indicate the average values while the lines indicate the standard deviation.

This preprint research paper has not been peer reviewed. Electronic copy available at: https://ssrn.com/abstract=4661637

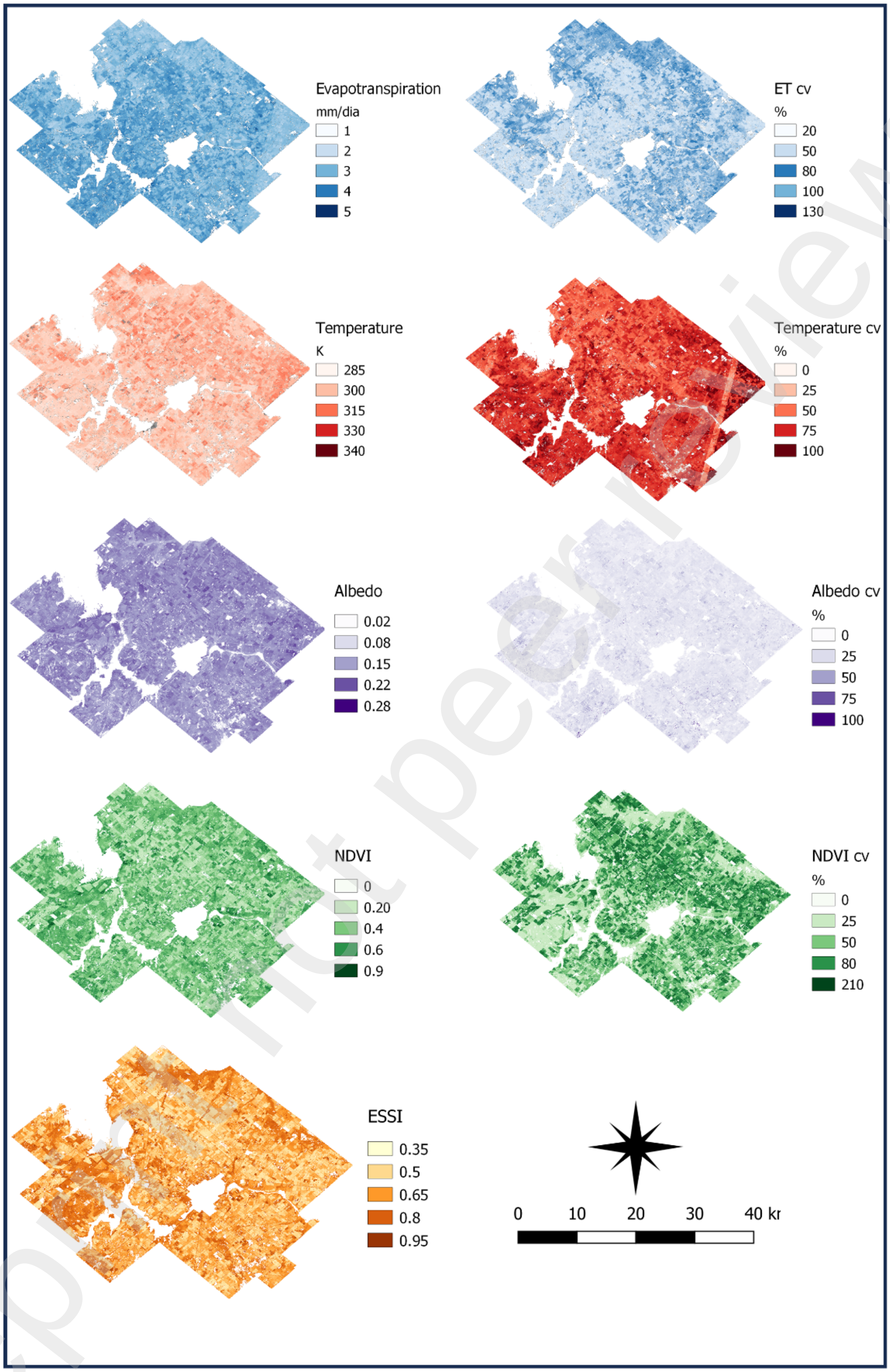

Figure 7. Spatial and intra-annual variation of the biophysical variables and calculated indicators: evapotranspiration, Land Surface Temperature, albedo, NDVI and ESSI. The maps on the left represent the average value along the growing season (July 2020 to June 2021), while the maps on the right represent the intra-annual coefficient of variation.

Preprint not peer reviewed

This preprint research paper has not been peer reviewed. Electronic copy available at: https://ssrn.com/abstract=4661637

The first two axes of the principal component analysis captured around 78% of the total variability of the biophysical variables. The Axis 1 explained 46.8% of the total variability, being NDVI, intra-annual coefficient of variation of NDVI and ESSI the most important variables (Figure 8). This axis allowed to differentiate the less productive and more seasonal cropping systems (single summer crops, dominated by soybean crops) from those more productive and less seasonal (double cropping and summer crops with cover crops) and from grasslands and pastures (Figure 8). The Axis 2 included biophysical variables associated with water dynamics and energy balance and their coefficient of variation. Thus, the ET, ETcv and albedocv turned out to be the most important variables in this axis (Figure 8). In this way, the double cropping showed highest ET and seasonality of albedo and intermediate values of ETcv. The summer crops with cover crops showed important differences with the double cropping, despite having a similar soil cover in the growth period. Thereby, they showed more similar values of ET, ETcv and productivity respect to grassland (Figure 8).

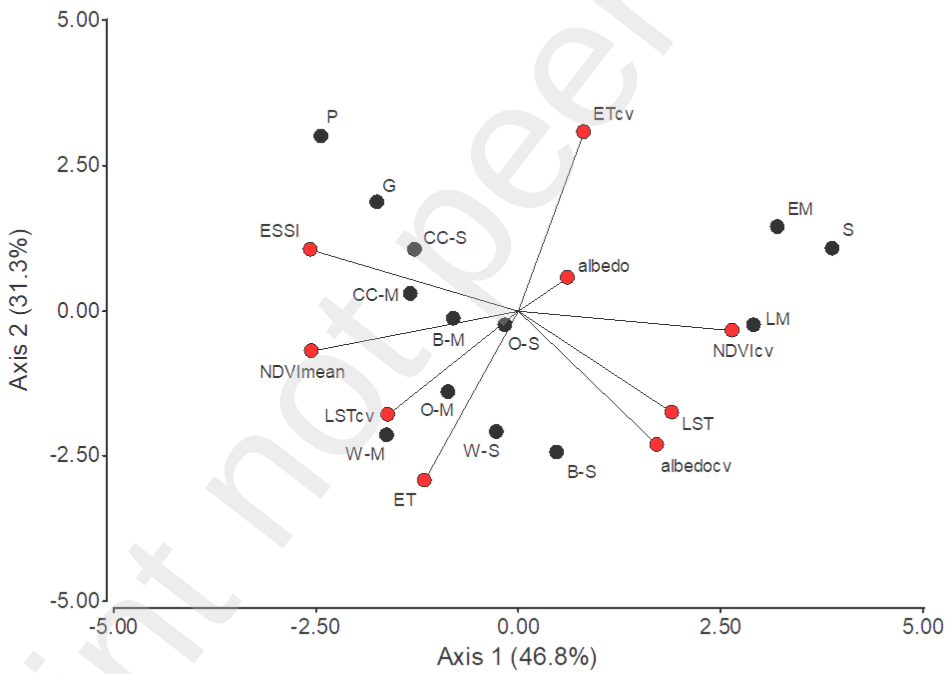

Figure 8. Biplot derived from a principal component analysis run on R. The black dots indicate the distribution of the different cropping systems (W-M: wheat-maize, W-S: wheat-soybean, P: pasture, B-M: barley-maize, B-S: barley-soybean, O-M: oat-maize, O-S: oat-soybean, EM: early maize, LM: late maize, S: soybean, CC-S: cover crop-soybean, CC-M: cover crop-maize, G: grassland). while the lines with red dots indicate the eigenvectors of the biophysical variables. It is observed that 46.8% of the variability between the cropping systems (Axis 1) is mainly associated with the NDVIcv in contrast to the NDVImean and the ESSI. The Axis 2 explains 31.3% of the variability and is mainly associated with ETcv in contrast to ETmean and, to a lesser extent, with LST and albedo.

Preprint not peer reviewed

This preprint research paper has not been peer reviewed. Electronic copy available at: https://ssrn.com/abstract=4661637

4. Discussion

The different crop types were identified with high precision, showing an F1-score always higher than 81% and 90% for the winter/spring and spring/summer season classifications, respectively. The overall accuracy or global F1-score of both classifications was 0.846 and 0.946, respectively, similar to those obtained with classical methods for the same region (Guershman et al. 2003, Baeza et al. 2014, Baeza and Paruelo 2020, De Abelleyra et al. 2020, De Abelleyra and Veron 2020, MapBiomas Pampa project (https://.pampa.mapbiomas.org, Baeza et al. 2022)). However, our work presents a classification with a higher thematic classes and spatial resolution (10-meter). Such increase in conceptual and spatial resolution would results in better estimates of crop systems areas. In fact, the estimated area covered by each crop from our classification was strongly correlated with those reported by MAGyP for barley, oat, maize, soybean, second soybean, wheat and other crops for Junín department for the 2020/2021 growing season ($r = 0.99$, p-value < 0.0001, RMSE = 3452 ha), which further supports the reliability of our classifications. Thus, our classifications improve available maps based on Landsat or MODIS images. These land use land cover classifications did not differentiate within winter or summer crop types. The Crops National Map (Mapa Nacional de Cultivos) generated annually by INTA since 2018 (De Abelleyra et al. 2020) is the available product with the highest conceptual resolution though it does not discriminate among different winter crops nor cover crops from double copping systems, and it does not identify pastures.

Cropping systems can play an important role in the mitigation of climate change and the counterbalance of global warming, through changing the radiation budget and reducing the radiative forcing through increase of the surface albedo (Betts et al. 2007, Ward et al. 2014, Davin et al. 2007, Ward and Mahowald 2015). The increase in albedo can partly offset the positive effect of greenhouse gas emissions (CO_2, CH_4, N_2O, etc) some agricultural activities cause due to fertilizer application and soil modification, among others (Robertson et al. 2000, Ward et al. 2014). In our study, cropping systems increased the albedo between 1.64 and 16.35% in comparison to grasslands, with single soybean crops showing one of the highest albedo values. Similar results were observed by Houspanossian et al. (2017) in the dry subtropical Chaco forests of Argentina with increases between 1 and 7% in albedo when converting pastures to agricultural crops. Also, higher values in single summer crops than in double cropping was observed, which was associated with higher soil brightness during fallow. However, the pattern observed in our work was contrary to what has been observed in various studies carried out in the northern hemisphere. These works show that the inclusion of covers and winter crops during fallow increase surface albedo (Kaye and Quemada 2017, Carrer et al. 2018, Lugato et al. 2020, McNellis et al. 2020, Liu et al. 2021), being even higher when the crop is maintained for a longer period (Carrer et al 2018), associated with a higher brightness

This preprint research paper has not been peer reviewed. Electronic copy available at: https://ssrn.com/abstract=4661637

of vegetation than of bare soils. Despite we observed that all cropping systems increased albedo compared to grasslands, single summer crops and mainly those that included soybeans, were the ones that presented the highest albedo. In the same way that observed in our work, preliminary results of an experiment located in La Estanzuela Experimental Station (National Institute for Agricultural Research [INIA], the Uruguayan National Agricultural Research Institute) located in southwestern Uruguay (34°20′ S, 57°41′ W; 82 masl) that evaluate environmental and productive performance along an agricultural intensification gradient show that summer cropping (soybean) presents a higher albedo than double cropping (wheat-soybean) and summer crops with cover crops, averaging 0.15, 0.10 and 0.13, respectively (Camba Sans, unpublished data). While the magnitude of the increased albedo from incorporating cover and winter crops was similar to findings in previous studies (equivalent here to a removal of 0.8–3.9 Mg CO_2eq ha^{-1} (Carrer et al. 2018, Lugato et al. 2020)), the net effect on carbon balance varies depending on the region and the average incident radiation. In comparison to all cropping systems, pastures exhibited a lower mean and seasonal variation of albedo than grasslands, likely due to a higher average leaf area index throughout the growing season (Kalma and Badham 1972). This was evident in the observation that pastures showed higher average NDVI values compared to grasslands.

Anthropogenic land cover changes may also modify climate through altering sensible and latent heat fluxes (Marshall et al. 2004, Pielke et al. 2007). Some studies based on MODIS land surface temperature showed opposite impacts of agriculture on surface temperature depending on the analyzed moment of the growing season. In general, a cooling effect was observed during the growing season in crops compared to natural cover, but a warming effect was observed after harvest (Ge 2010, Wei et al. 2021). This is coincident with our observed increase of seasonal variation of temperature for the different cropping systems compared to grasslands. In addition, we observed a warming trend at an annual timescale, as previously for some regions (Wei et al. 2021). All cropping systems, except for pastures, showed higher Land Surface Temperatures (LST) than grasslands, indicating a local warming effect after grassland conversion. LST differences were 6.67 ± 3.79 °K (mean ± SD), similar to the warming caused by deforestation (Sabajo et al. 2017). Higher LST in agricultural lands compared to grassland contrast with the lower radiation load resulting from the higher albedo, although no significant correlation was observed between both variables. So, the potential surface cooling from increased albedo is offset by warming from decreased sensitive heat fluxes, with the net effect being a surface warming (Luyssaert et al. 2014). Thus, croplands would have a negative effect on the global warming through the reduction of the radiative forcing because of the increase of the surface albedo at global scale and, in turn, a positive effect on the surface temperature on a local or regional scale.

This preprint research paper has not been peer reviewed. Electronic copy available at: https://ssrn.com/abstract=4661637

Preprint not peer reviewed

The double cropping was the only cropping system that showed higher ET values than grasslands. Summer crops with cover crops showed very similar values, although those with maize showed slightly higher values and those with soybeans showed slightly lower values. In turn, the different cropping systems presented a high seasonal variation of ET, except for summer crops. The higher evapotranspiration rates observed in double cropping compared to single summer crops match with those observed by Nosetto et al. (2015), reaching annual differences close to 100 mm. At the same time, Olivera Rodriguez et al. (2021) also recorded lower ET in soybean crops compared to reference ET. However, the higher thematic resolution of our cropping system classification allowed us to differentiate crop types and thus to separate into double cropping, single summer crops and single summer crops with cover crops, and within them, those that presented maize from those that contained soybean. Thus, cropping systems with soybean as a summer crop showed, on average, 26 mm less of annual ET, with maximum differences of up to 74 mm compared to those that presented maize. Replacement of grasslands by croplands is known to cause noticeable hydrological alterations (Nosetto et al. 2015). The replacement of grasslands by the double cropping led to minor hydrological changes, but single summer crops significantly reduced evapotranspiration and increased hydrological flow (Nosetto et al. 2015). These excesses of liquid water could enhance recharge and raise groundwater levels, potentially triggering flooding (Aragón et al., 2010), as has been reported in the Inland Pampas of Argentina (Viglizzo et al., 2009). In fact, a recent study determined that the expansion of agriculture is causing greater floods in the South American plains, caused by a decline in rooting depth and in evapotranspiration in croplands (Houspanossian et al. 2023). Our findings indicate potential negative hydrological impacts that may be mitigated through the adoption of double cropping or summer crops with cover crops instead of the current single crop system. The single crop system currently covers approximately 40% of the region under study and 60% of the sown area. Implementing these alternative cropping practices could help alleviate the identified hydrological issues.

The ecosystem services supply index (ESSI) was higher in those cropping systems that presented more than one crop in the growing season and, in turn, when at least one of the crops was not harvested for grain, as in the case of pastures or summer crops with cover crops. Thus, these cropping systems would allow the maintenance and even slight increase of the ecosystem services supply related to both carbon and water dynamics compared to natural grasslands. Pastures or summer crops with cover crops presented a similar average annual productivity, so the higher ESSI values of the pastures would be associated with their lower seasonality. On the other hand, doubles cropping showed a similar annual net primary productivity (as assessed from NDVI) and even higher than that reported by summer crops with cover crops and grasslands but showed a reduction in the ESSI close to 10%. This ESSI reduction in double cropping can be explained by, on the one hand, to its greater seasonality and, on the other hand, to its agricultural

This preprint research paper has not been peer reviewed. Electronic copy available at: https://ssrn.com/abstract=4661637

Preprint not peer reviewed

management. Cover crops, unlike winter crops, are seeded between cash crops and are not harvested nor incorporated into the soil as green manure, and also not intended for grazing like annual forage (Rimski- Korsakov et al. 2015). On the other hand, single summer crops showed a reduction close to 22% of the ESSI compared to grasslands. In agreement with our work, where we observed an average reduction in ESSI close to 17%, Paruelo et al. (2022) observed an average difference between grassland and transformed land cover ranging from 15 to 22%. Similarly, Rositano et al. (2022) observed that the counties of the Pampa region that had the largest area under soybean cultivation were associated with relatively high loss of ESSI. This decrease in ESSI would have negative consequences on soil organic carbon content (Staiano et al. 2021, Baldassini et al. 2023), avian diversity and abundance (Weyland et al. 2019), groundwater recharge and evapotranspiration (Paruelo et al. 2016). The ESSI allows capturing differences in C inputs associated with land use and land cover (Staiano et al. 2021) and agricultural rotations (Baldassini et al. 2023) thus being a good indicator of SOC stocks variations. Thus, the replacement of natural covers by agriculture and agricultural rotations with a lower proportion of pastures showed lower values of ESSI and organic carbon in the soil (Staiano et al. 2021, Baldassini et al. 2023). Regarding ET, Paruelo et al. (2016) observed a positive relationship between the ESSI and evapotranspiration, where close to 52% of the ET variance was explained by ESSI. However, in our work we did not find a significant linear correlation between both variables, although both presented a quadratic relationship (ET(mm/day)=-36.33*ESSI^2+47.24*ESSI-12.14, p-value=0.0092, R^2 =0.61). Thus, ET was maximum for intermediate values of ESSI, which corresponded to double cropping. Single summer crops showed the lowest ET and the lowest ESSI values by presenting a lower NDVImean and a higher NDVIcv. Summer crops with cover crops, pastures and natural grasslands showed the highest ESSI values, presenting high NDVImean (similar to double crops) and low NDVIcv (lower than double crops), although intermediate ET values.

5. Final remarks

Due to the dissimilar impacts of the different cropping systems on the biophysical variables and on ecosystem services supply, our results support the benefits from preserving and expanding the area covered by production systems that keep the soil covered for most of the year. Thus, schemes based on summer crops with cover crops and pastures would allow maintaining ecosystem functioning similar to native grasslands. Despite the multiple benefits provided by cover crops (Varela et al. 2014, Blanco-Canqui et al. 2015, Alvarez et al. 2017, Landriscini et al. 2019, Fontana et al. 2021), they were seldom included in annual rotations. They represented less than 1% in the study area, preceding soybean (the main rainfed crop type in the study area, Ministerio de

Preprint not peer reviewed
This preprint research paper has not been peer reviewed. Electronic copy available at: https://ssrn.com/abstract=4661637

Agroindustria, 2017; https://datos.agroindustria.gob.ar/dataset/ estimates-agricultural) and maize, perhaps because of their water consumption which could affect cash crops development and final yield of the summer crops (Pinto et al. 2017, Alvarez et al. 2017).

This study represents an important improvement with respect to previous works since it was possible to characterize different cropping systems with adequate precision and to estimate their impact on biophysical variables and ecosystem services supply with a higher spatial resolution than before. In recent years, most of the applications of ESSI were oriented to provide a quantitative diagnosis and monitoring over areas subjected to land cover transformation or degradation due to overgrazing based on information provided by the MODIS sensor (Staiano et al. 2021). Undoubtedly, this work is a new case of application on productive areas with a higher spatial resolution, thus providing key information for decision-making and territorial planning. Although our study was confined to a limited area, our results can be extrapolated for the whole RPG region (~820,000 km^2) which becomes relevant at the regional level since approximately half of the area is covered by agricultural crops (Hall et al. 1992, Soriano 1992, Burkart et al. 1998). However, our analysis was limited to 2020-2021 growing season, when specific climatic conditions may have influenced our results. Characterizing the main crop sequences or rotations over years (e.g., De Abelleyra and Veron 2020) and the level of agricultural intensification (e.g., considering the frequency with which soybean are planted along years (Song et al. 2021)) would allow further analysis by considering climatic variations and agricultural managements for the agricultural Pampean region of Argentina. Facilitating access to field data with land cover records is key for expanding this analysis to a regional level and for a longer time range.

6. Acknowledgments

This research was supported by UBA, CONICET and FONCyT-PICT 2020-SERIEA-01321. Also, this work was carried out with the financial aid of the Asociación Universitaria Iberoamericana de Postgrado (AUIP) and the program “Estancias de Investigadores de otros Centros Nacionales y Extranjeros en Departamentos e Institutos o Centros de Investigación de la Universidad de Granada” from the University of Granada and by the support of the Consejería de Economía, Conocimiento, Empresas y Universidad de la Junta de Andalucía. DAS acknowledges support from the EarthCul Project (reference PID2020-118041GB-I00), funded by the Spanish Ministry of Science and Innovation and from the “Thematic Center on Mountain Ecosystem & Remote sensing, Deep learning-AI e-Services University of Granada-Sierra Nevada” (LifeWatch-2019-10-UGR-4), which has been co-funded by the Ministry of Science and Innovation through the FEDER funds

Preprint not peer reviewed

This preprint research paper has not been peer reviewed. Electronic copy available at: https://ssrn.com/abstract=4661637

from the Spanish Pluriregional Operational Program 2014-2020 (POPE), LifeWatch-ERIC action line. We also thank MAGyP for sharing the field data for this work.

7. References

Alcaraz-Segura, D., Paruelo, J. M., Epstein, H. E., & Cabello, J. (2013). Environmental and human controls of ecosystem functional diversity in temperate South America. Remote Sensing, 5(1), 127-154.

Altesor, A., Gallego, F., Ferrón, M., Pezzani, F., López-Mársico, L., Lezama, F., ... & Paruelo, J. M. (2019). Inductive approach to build state-and-transition models for Uruguayan Grasslands. Rangeland Ecology & Management, 72(6), 1005-1016.

Alvarez, R., Steinbach, H. S., & De Paepe, J. L. (2017). Cover crop effects on soils and subsequent crops in the pampas: A meta-analysis. Soil and Tillage Research, 170, 53-65.

Aragón, R., Jobbágy, E. G., & Viglizzo, E. F. (2011). Surface and groundwater dynamics in the sedimentary plains of the Western Pampas (Argentina). Ecohydrology, 4(3), 433-447.

Baeza, S., and Paruelo, J. M. (2020). Land use/land cover change (2000–2014) in the Rio de la Plata grasslands: an analysis based on MODIS NDVI time series. Remote sensing, 12(3), 381.

Baeza, S., Baldassini, P., Bagnato, C., Pinto, P., & Paruelo, J. (2014). Caracterización del uso/cobertura del suelo en Uruguay a partir de series temporales de imágenes MODIS. Agrociencia (Uruguay), 18(2), 95-105.

Baeza, S., Vélez-Martin, E., De Abelleyra, D., Banchero, S., Gallego, F., Schirmbeck, J., ... & Hasenack, H. (2022). Two decades of land cover mapping in the Río de la Plata grassland region: The MapBiomas Pampa initiative. Remote Sensing Applications: Society and Environment, 28, 100834.

Bala G, Caldeira K, Wickett M, Phillips TJ, Lobell DB, Delire C, Mirin A (2007) Combined climate and carbon-cycle effects of large-scale deforestation. Proc Natl Acad Sci USA 104:6550–6555

Baldassini, P., Baethgen, W., Camba-Sans, G.H., Quincke, A., Pravia, M. V., Terra, J., Macedo, I., Piñeiro, G., and Paruelo, J. M.; Carbon stocks and potential sequestration of Uruguayan soils. A road map to a comprehensive characterization of temporal and spatial

Preprint not peer reviewed

This preprint research paper has not been peer reviewed. Electronic copy available at: https://ssrn.com/abstract=4661637

changes to assess Carbon footprint, Front. Sustainable Food Syst., 7, 1045734, https://doi.org/10.3389/fsufs.2023.1045734, 2023.

Baldi, G., and Paruelo, J. M. (2008). Land-use and land cover dynamics in South American temperate grasslands. Ecology and Society, 13(2).

Baldi, G., Nosetto, M. D., Aragón, R., Aversa, F., Paruelo, J. M., & Jobbágy, E. G. (2008). Long-term satellite NDVI data sets: evaluating their ability to detect ecosystem functional changes in South America. Sensors, 8(9), 5397-5425.

Bargiel, D. (2017). A new method for crop classification combining time series of radar images and crop phenology information. Remote sensing of environment, 198, 369-383.

Betts, R. A., Falloon, P. D., Goldewijk, K. K., & Ramankutty, N. (2007). Biogeophysical effects of land use on climate: Model simulations of radiative forcing and large-scale temperature change. Agricultural and forest meteorology, 142(2-4), 216-233.

Blanco-Canqui, H., Shaver, T. M., Lindquist, J. L., Shapiro, C. A., Elmore, R. W., Francis, C. A., & Hergert, G. W. (2015). Cover crops and ecosystem services: Insights from studies in temperate soils. Agronomy journal, 107(6), 2449-2474.

Bonan, G. B. (2004). Biogeophysical feedbacks between land cover and climate. Washington DC American Geophysical Union Geophysical Monograph Series, 153, 61-72.

Brown, C. F., Brumby, S. P., Guzder-Williams, B., Birch, T., Hyde, S. B., Mazzariello, J., ... & Tait, A. M. (2022). Dynamic World, Near real-time global 10 m land use land cover mapping. Scientific Data, 9(1), 251.

Buchhorn, M., Lesiv, M., Tsendbazar, N. E., Herold, M., Bertels, L., & Smets, B. (2020). Copernicus global land cover layers—collection 2. Remote Sensing, 12(6), 1044.

Camba Sans, G. H., Verón, S. R., & Paruelo, J. M. (2021). Forest strips increase connectivity and modify forests' functioning in a deforestation hotspot. Journal of Environmental Management, 290, 112606.

Campbell, J. L., Driscoll, C. T., Eagar, C., Likens, G. E., Siccama, T. G., Johnson, C. E., ... & Buso, D. C. (2007). Long-term trends from ecosystem research at the Hubbard Brook Experimental Forest. Gen. Tech. Rep. NRS-17. Newtown Square, PA: US Department of Agriculture, Forest Service, Northern Research Station. 41 p., 17.

Carlson, T. N., Capehart, W. J., & Gillies, R. R. (1995). A new look at the simplified method for remote sensing of daily evapotranspiration. Remote sensing of Environment, 54(2), 161-167.

Preprint not peer reviewed

This preprint research paper has not been peer reviewed. Electronic copy available at: https://ssrn.com/abstract=4661637

Carrer D, Pique G, Ferlicoq M, Ceamanos X, Ceschia E 2018. What is the potential of cropland albedo management in the fight against global warming? A case study based on the use of cover crops. Environmental Research Letters 13: 1-11

Caselles, V., Artigao, M. M., Hurtado, E., Coll, C., & Brasa, A. (1998). Mapping actual evapotranspiration by combining Landsat TM and NOAA-AVHRR images: application to the Barrax area, Albacete, Spain. Remote Sensing of Environment, 63(1), 1-10.

Chapin III, F. S., Matson, P. A., & Vitousek, P. (2011). Principles of terrestrial ecosystem ecology. Springer Science & Business Media.

Chuvieco, E. (1990). Fundamentos de teledetección espacial.

Davin, E. L., Seneviratne, S. I., Ciais, P., Olioso, A., & Wang, T. (2014). Preferential cooling of hot extremes from cropland albedo management. Proceedings of the National Academy of Sciences, 111(27), 9757-9761.

de Abelleyra, D., and Verón, S. (2020). Crop rotations in the Rolling Pampas: Characterization, spatial pattern and its potential controls. Remote Sensing Applications: Society and Environment, 18, 100320.

De Abelleyra, D., Veron, S., Banchero, S., Mosciaro, M. J., Propato, T., Ferraina, A., ... & Volante, J. (2020, March). First large extent and high resolution cropland and crop type map of Argentina. In 2020 IEEE Latin American GRSS & ISPRS Remote Sensing Conference (LAGIRS) (pp. 392-396). IEEE.

De Groot, R. S., Alkemade, R., Braat, L., Hein, L., & Willemen, L. (2010). Challenges in integrating the concept of ecosystem services and values in landscape planning, management and decision making. Ecological complexity, 7(3), 260-272.

Deschamps, B., McNairn, H., Shang, J., & Jiao, X. (2012). Towards operational radar-only crop type classification: comparison of a traditional decision tree with a random forest classifier. Canadian Journal of Remote Sensing, 38(1), 60-68.

Di Bella, C. M., Rebella, C. M., & Paruelo, J. M. (2000). Evapotranspiration estimates using NOAA AVHRR imagery in the Pampa region of Argentina. International Journal of Remote Sensing, 21(4), 791-797.

Fisher, B., Turner, R. K., & Morling, P. (2009). Defining and classifying ecosystem services for decision making. Ecological economics, 68(3), 643-653.

Foerster, S., Kaden, K., Foerster, M., & Itzerott, S. (2012). Crop type mapping using spectral–temporal profiles and phenological information. Computers and Electronics in Agriculture, 89, 30-40.

Preprint not peer reviewed

This preprint research paper has not been peer reviewed. Electronic copy available at: https://ssrn.com/abstract=4661637

Foley JA et al (2005) Global consequences of land use. Science 309(5734):570–574

Fontana, M. B., Novelli, L. E., Sterren, M. A., Uhrich, W. G., Benintende, S. M., & Barbagelata, P. A. (2021). Long-term fertilizer application and cover crops improve soil quality and soybean yield in the Northeastern Pampas region of Argentina. Geoderma, 385, 114902.

Foody, G.M., Mcculloch, M.B. and Yates, W.B., 1994, Crop classification from C-band polarimetric radar data. International Journal of Remote Sensing, 15, pp. 2871–2885.

Friedl, M. A., Sulla-Menashe, D., Tan, B., Schneider, A., Ramankutty, N., Sibley, A., & Huang, X. (2010). MODIS Collection 5 global land cover: Algorithm refinements and characterization of new datasets. Remote sensing of Environment, 114(1), 168-182.

Gallego, F., Paruelo, J. M., Baeza, S., & Altesor, A. (2020). Distinct ecosystem types respond differentially to grazing exclosure. Austral Ecology, 45(5), 548-556.

Gallego, F., Sans, G. C., Di Bella, C. M., Tiscornia, G., & Paruelo, J. M. (2023). Performance of real evapotranspiration products and water yield estimations in Uruguay. Remote Sensing Applications: Society and Environment, 101043.

Ge, J. (2010). MODIS observed impacts of intensive agriculture on surface temperature in the southern Great Plains. International Journal of Climatology, 30(13), 1994-2003.

Giri, C., and Long, J. (2014). Land cover characterization and mapping of South America for the year 2010 using Landsat 30 m satellite data. Remote sensing, 6(10), 9494-9510.

Gitelson, A.A., Y.J. Kaufman, and M.N. Merzlyak, 1996. Use of a green channel in remote sensing of global vegetation from EOS-MODIS. Remote Sens. Environ. 58:289-298.

Gorelick, N., Hancher, M., Dixon, M., Ilyushchenko, S., Thau, D., & Moore, R. (2017). Google Earth Engine: Planetary-scale geospatial analysis for everyone. Remote sensing of Environment, 202, 18-27.

Granger, R. J. (2000). Satellite-derived estimates of evapotranspiration in the Gediz basin. Journal of Hydrology, 229(1-2), 70-76.

Guerschman, J. P., Paruelo, J. M., Bella, C. D., Giallorenzi, M. C., & Pacin, F. (2003). Land cover classification in the Argentine Pampas using multi-temporal Landsat TM data. International Journal of Remote Sensing, 24(17), 3381-3402.

Haack, B., and Bechdol, M. (2000). Integrating multisensor data and RADAR texture measures for land cover mapping. Computers & Geosciences, 26(4), 411-421.

Preprint not peer reviewed

This preprint research paper has not been peer reviewed. Electronic copy available at: https://ssrn.com/abstract=4661637

Hall, A. J., Rebella, C. M., Ghersa, C. M., & Culot, J. P. (1992). Field-crop systems of the Pampas In: Pearson CJ (ed) Ecosystems of the world. Field crop ecosystems.

Hannah, L., Carr, J. L., & Lankerani, A. (1995). Human disturbance and natural habitat: a biome level analysis of a global data set. Biodiversity & Conservation, 4, 128-155.

Hardisky MA, Klemas V, Smart RM (1983) The influence of soil salinity, growth form, and leaf moisture on-the spectral radiance of ~Spartina alterniflora canopies. Photogramm Eng Remote Sensing 49(1):77–83

Hoekstra, J. M., Boucher, T. M., Ricketts, T. H., & Roberts, C. (2005). Confronting a biome crisis: global disparities of habitat loss and protection. Ecology letters, 8(1), 23-29.

Houspanossian, J., Giménez, R., Jobbágy, E., & Nosetto, M. (2017). Surface albedo raise in the South American Chaco: Combined effects of deforestation and agricultural changes. Agricultural and Forest Meteorology, 232, 118-127.

Houspanossian, J., Giménez, R., Whitworth-Hulse, J. I., Nosetto, M. D., Tych, W., Atkinson, P. M., ... & Jobbágy, E. G. (2023). Agricultural expansion raises groundwater and increases flooding in the South American plains. Science, 380(6652), 1344-1348.

Hu, B., Xu, Y., Huang, X., Cheng, Q., Ding, Q., Bai, L., & Li, Y. (2021). Improving urban land cover classification with combined use of sentinel-2 and sentinel-1 imagery. ISPRS International Journal of Geo-Information, 10(8), 533.

Huete, A., Didan, K., Miura, T., Rodriguez, E. P., Gao, X., & Ferreira, L. G. (2002). Overview of the radiometric and biophysical performance of the MODIS vegetation indices. Remote sensing of environment, 83(1-2), 195-213.

Hugh D. E., Belward, A. S., De Miranda, E. E., Di Bella, C. M., Gond, V., Huber, O., ... & Fritz, S. (2004). A land cover map of South America. Global Change Biology, 10(5), 731-744.

INTA (2018). https://inta.gob.ar/unidades/213000/cartografia-genesis-y-evaluacion-de-tierras (June 2018)

Jackson, R. D. (1985). Evaluating evapotranspiration at local and regional scales. Proceedings of the IEEE, 73(6), 1086-1096.

Jackson, R. D., Reginato, R. J., & Idso, S. (1977). Wheat canopy temperature: a practical tool for evaluating water requirements. Water resources research, 13(3), 651-656.

Jobbágy, E. G., Nosetto, M., Paruelo, J. M., & Piñeiro, G. (2006). Las forestaciones rioplatenses y el agua. Ciencia Hoy, 16(95), 12-21.

Preprint not peer reviewed

This preprint research paper has not been peer reviewed. Electronic copy available at: https://ssrn.com/abstract=4661637

Jullian, C., Nahuelhual, L., & Laterra, P. (2021). The Ecosystem Service Provision Index as a generic indicator of ecosystem service supply for monitoring conservation targets. Ecological Indicators, 129, 107855.

Kalma, J. D., and Badham, R. (1972). The radiation balance of a tropical pasture, I. The reflection of short-wave radiation. Agricultural Meteorology, 10, 251-259.

Kaye, J. P., and Quemada, M. (2017). Using cover crops to mitigate and adapt to climate change. A review. Agronomy for sustainable development, 37, 1-17.

Kent, Federico (ed.). 2019. Forrajeras cultivadas anuales y perennes más difundidas en la provincia de La Pampa. La Pampa : Ediciones INTA. p. 57-64

Key, C. H., and Benson, N. C. (1999, June). Measuring and remote sensing of burn severity. In Proceedings joint fire science conference and workshop (Vol. 2, p. 284). University of Idaho and International Association of Wildland Fire Moscow, ID.

Kite, G. W., & Pietroniro, A. (1996). Remote sensing applications in hydrological modelling. Hydrological Sciences Journal, 41(4), 563-591.

Kpienbaareh, D., Sun, X., Wang, J., Luginaah, I., Bezner Kerr, R., Lupafya, E., & Dakishoni, L. (2021). Crop type and land cover mapping in northern Malawi using the integration of sentinel-1, sentinel-2, and planetscope satellite data. Remote Sensing, 13(4), 700.

Lambin, E. F., and Meyfroidt, P. (2011). Global land use change, economic globalization, and the looming land scarcity. Proceedings of the National Academy of Sciences, 108(9), 3465-3472.

Landriscini, M. R., Galantini, J. A., Duval, M. E., & Capurro, J. E. (2019). Nitrogen balance in a plant-soil system under different cover crop-soybean cropping in Argentina. Applied Soil Ecology, 133, 124-131.

Lawrence, D., Coe, M., Walker, W., Verchot, L., & Vandecar, K. (2022). The unseen effects of deforestation: biophysical effects on climate. Frontiers in Forests and Global Change, 5, 49.

León, R. J. C., Sala, O. E., Lavado, R. S., & Deregibus, V. A. (1991). Río de la Plata grasslands. Natural grasslands: introduction and western hemisphere. Ecosystems of the World. Elsevier, Amsterdam, 369-376.

Li, W., Fu, H., Yu, L., Gong, P., Feng, D., Li, C., & Clinton, N. (2016). Stacked Autoencoder-based deep learning for remote-sensing image classification: a case study of African land-cover mapping. International journal of remote sensing, 37(23), 5632-5646.

Preprint not peer reviewed

This preprint research paper has not been peer reviewed. Electronic copy available at: https://ssrn.com/abstract=4661637

Liang, S. (2000). Numerical experiments on the spatial scaling of land surface albedo and leaf area index. Remote Sensing Reviews, 19(1-4), 225-242.

Liu, J., Desjardins, R. L., Wang, S., Worth, D. E., Qian, B., & Shang, J. (2022). Climate impact from agricultural management practices in the Canadian Prairies: Carbon equivalence due to albedo change. Journal of Environmental Management, 302, 113938.

Lloyd, D. (1990). A phenological classification of terrestrial vegetation cover using shortwave vegetation index imagery. TitleREMOTE SENSING, 11(12), 2269-2279.

Los, S. O., Pollack, N. H., Parris, M. T., Collatz, G. J., Tucker, C. J., Sellers, P. J., ... & Dazlich, D. A. (2000). A global 9-yr biophysical land surface dataset from NOAA AVHRR data. Journal of hydrometeorology, 1(2), 183-199.

Lovett, G. M., C. G. Jones, M. G. Turner, and K. C. Weathers. 2006. Ecosystem function in heterogeneous landscapes. Pp. 1–4 in G. M. Lovett, C. G. Jones, M. G. Turner and K. C. Weathers, eds. Ecosystem function in heterogeneous landscapes. Springer, New York.

Lugato, E., Cescatti, A., Jones, A., Ceccherini, G., & Duveiller, G. (2020). Maximising climate mitigation potential by carbon and radiative agricultural land management with cover crops. Environmental Research Letters, 15(9), 094075.

Luyssaert, S., Jammet, M., Stoy, P. C., Estel, S., Pongratz, J., Ceschia, E., ... & Dolman, A. J. (2014). Land management and land-cover change have impacts of similar magnitude on surface temperature. Nature Climate Change, 4(5), 389-393.

Mahmood, R., Pielke Sr, R. A., Hubbard, K. G., Niyogi, D., Dirmeyer, P. A., McAlpine, C., ... & Fall, S. (2014). Land cover changes and their biogeophysical effects on climate. International journal of climatology, 34(4), 929-953.

Marcos, B., Gonçalves, J., Alcaraz-Segura, D., Cunha, M., & Honrado, J. P. (2023). Assessing the resilience of ecosystem functioning to wildfires using satellite-derived metrics of post-fire trajectories. Remote Sensing of Environment, 286, 113441.

Marshall, C. H., Pielke, R. A., Steyaert, L. T., & Willard, D. A. (2004). The impact of anthropogenic land-cover change on the Florida peninsula sea breezes and warm season sensible weather. Monthly Weather Review, 132(1), 28-52.

Maxwell, K., Rajabi, M., & Esterle, J. (2019). Automated classification of metamorphosed coal from geophysical log data using supervised machine learning techniques. International Journal of Coal Geology, 214, 103284.

Preprint not peer reviewed

This preprint research paper has not been peer reviewed. Electronic copy available at: https://ssrn.com/abstract=4661637

McNaughton, S. J., Oesterheld, M., Frank, D. A., & Williams, K. J. (1989). Ecosystem-level patterns of primary productivity and herbivory in terrestrial habitats. Nature, 341(6238), 142-144.

Mcnellis, R. (2020). Leaf traits drive increases in albedo and latent heat flux of winter cover crops in Texas agricultural systems (Doctoral dissertation).

Milkovic, M., Michelson, A., Miñarro, F., Lanz, I., & Jaramillo, M. (2016). La salud de nuestra Tierra. Fundación Vida Silvestre Argentina. Available in: https://www. vidasilvestre. org. ar/sala_redaccion/opublicaciones, 16580.

Milkovic, M., Paruelo, J. M., & Nosetto, M. D. (2019). Hydrological impacts of afforestation in the semiarid Patagonia: A modelling approach. Ecohydrology, 12(6), e2113.

Ministerio de Agricultura Ganaderia y Pesca (MAGYP). 2016. Metodo de Segmentos Aleatorios: Metodología para la Estimación de la Superficie Sembrada con Cultivos Extensivos. Version V. Taken from https://www.magyp.gob.ar/sitio/areas/estimaciones/acerca_de/metodologia/_archivos/000000_M etodo-de-segmentos-aleatorios-Version-5.pdf

Modernel, P., Rossing, W. A., Corbeels, M., Dogliotti, S., Picasso, V., & Tittonell, P. (2016). Land use change and ecosystem service provision in Pampas and Campos grasslands of southern South America. Environmental Research Letters, 11(11), 113002.

Monteith, J. L. (1972). Solar radiation and productivity in tropical ecosystems. Journal of applied ecology, 9(3), 747-766.

Moran, M. S., and Jackson, R. D. (1991). Assessing the spatial distribution of evapotranspiration using remotely sensed inputs. Journal of Environmental Quality, 20(4), 725-737.

Mu, Q., Heinsch, F. A., Zhao, M., & Running, S. W. (2007). Development of a global evapotranspiration algorithm based on MODIS and global meteorology data. Remote sensing of Environment, 111(4), 519-536.

Murthy, C. S., Raju, P. V., & Badrinath, K. V. S. (2003). Classification of wheat crop with multi-temporal images: Performance of maximum likelihood and artificial neural networks. International Journal of Remote Sensing, 24(23), 4871-4890.

Myhre, G., and Myhre, A. (2003). Uncertainties in radiative forcing due to surface albedo changes caused by land-use changes. Journal of Climate, 16(10), 1511-1524.

Nemani, R., and Running, S. (1997). Land cover characterization using multitemporal red, near-IR, and thermal-IR data from NOAA/AVHRR. Ecological applications, 7(1), 79-90.

This preprint research paper has not been peer reviewed. Electronic copy available at: https://ssrn.com/abstract=4661637

Preprint not peer reviewed

Newbold, T., Hudson, L. N., Hill, S. L., Contu, S., Lysenko, I., Senior, R. A., ... & Purvis, A. (2015). Global effects of land use on local terrestrial biodiversity. Nature, 520(7545), 45-50.

Nosetto, M. D., Paez, R. A., Ballesteros, S. I., & Jobbágy, E. G. (2015). Higher water-table levels and flooding risk under grain vs. livestock production systems in the subhumid plains of the Pampas. Agriculture, Ecosystems & Environment, 206, 60-70.

Nosetto, M. D., Jobbágy, E. G., & Paruelo, J. M. (2005). Land-use change and water losses: the case of grassland afforestation across a soil textural gradient in central Argentina. Global Change Biology, 11(7), 1101-1117.

Olivera Rodriguez, P. O., Holzman, M. E., Degano, M. F., Faramiñán, A. M. G., Rivas, R. E., & Bayala, M. I. (2021). Spatial variability of the green water footprint using a medium-resolution remote sensing technique: The case of soybean production in the Southeast Argentine Pampas. Science of the Total Environment, 763, 142963.

Paruelo, J. M. (2008). La caracterización funcional de ecosistemas mediante sensores remotos. Ecosistemas, 17(3).

Paruelo, J. M., and Sierra, M. (2023). Sustainable intensification and ecosystem services: how to connect them in agricultural systems of southern South America. Journal of Environmental Studies and Sciences, 13(1), 198-206.

Paruelo, J. M., Oesterheld, M., Altesor, A., Piñeiro, G., Rodríguez, C., Baldassini, P., ... & Pillar, V. D. (2022). Grazers and fires: Their role in shaping the structure and functioning of the Río de la Plata Grasslands. Ecología Austral, 32(2bis), 784-805.

Paruelo, J. M., Jobbágy, E. G., & Sala, O. E. (2001). Current distribution of ecosystem functional types in temperate South America. Ecosystems, 4, 683-698.

Paruelo, J. M., Guerschman, J. P., & Verón, S. R. (2005). Expansión agrícola y cambios en el uso del suelo. Ciencia hoy, 15(87), 14-23.

Paruelo, J. M., Guerschman, J. P., Pineiro, G., Jobbagy, E. G., Verón, S. R., Baldi, G., & Baeza, S. (2006). Cambios en el uso de la tierra en Argentina y Uruguay: marcos conceptuales para su análisis. Agrociencia Uruguay, 10(2), 47-61.

Paruelo, J. M., Jobbágy, E. G., Oesterheld, M., Golluscio, R. A., & Aguiar, M. R. (2007). The grasslands and steppes of Patagonia and the Rio de la Plata plains. The physical geography of South America, 232-248.

Paruelo, J. M., Texeira, M., Staiano, L., Mastrángelo, M., Amdan, L., & Gallego, F. (2016). An integrative index of Ecosystem Services provision based on remotely sensed data. Ecological indicators, 71, 145-154.

Preprint not peer reviewed

This preprint research paper has not been peer reviewed. Electronic copy available at: https://ssrn.com/abstract=4661637

Pekel, J. F., Cottam, A., Gorelick, N., & Belward, A. S. (2016). High-resolution mapping of global surface water and its long-term changes. Nature, 540(7633), 418-422.

Song, X. P., Hansen, M. C., Potapov, P., Adusei, B., Pickering, J., Adami, M., ... & Tyukavina, A. (2021). Massive soybean expansion in South America since 2000 and implications for conservation. Nature sustainability, 4(9), 784-792.

Pielke Sr, R. A., Davey, C. A., Niyogi, D., Fall, S., Steinweg-Woods, J., Hubbard, K., ... & Blanken, P. (2007). Unresolved issues with the assessment of multidecadal global land surface temperature trends. Journal of Geophysical Research: Atmospheres, 112(D24).

Pielke Sr, R. A., Pitman, A., Niyogi, D., Mahmood, R., McAlpine, C., Hossain, F., ... & de Noblet, N. (2011). Land use/land cover changes and climate: modeling analysis and observational evidence. Wiley Interdisciplinary Reviews: Climate Change, 2(6), 828-850.

Pimm, S. L., and Raven, P. (2000). Extinction by numbers. Nature, 403(6772), 843-845.

Pinto, P., Long, M. E. F., & Piñeiro, G. (2017). Including cover crops during fallow periods for increasing ecosystem services: Is it possible in croplands of Southern South America?. Agriculture, Ecosystems & Environment, 248, 48-57.

Potter, C. S., Randerson, J. T., Field, C. B., Matson, P. A., Vitousek, P. M., Mooney, H. A., & Klooster, S. A. (1993). Terrestrial ecosystem production: A process model based on global satellite and surface data. Global biogeochemical cycles, 7(4), 811-841.

Prince, S. D. (1991). A model of regional primary production for use with coarse resolution satellite data. International Journal of Remote Sensing, 12(6), 1313-1330.

Qin, Z., Dall'Olmo, G., Karnieli, A., & Berliner, P. (2001). Derivation of split window algorithm and its sensitivity analysis for retrieving land surface temperature from NOAA-advanced very high resolution radiometer data. Journal of Geophysical Research: Atmospheres, 106(D19), 22655-22670.

Regos, A., Gonçalves, J., Arenas-Castro, S., Alcaraz-Segura, D., Guisan, A., & Honrado, J. P. (2022). Mainstreaming remotely sensed ecosystem functioning in ecological niche models. Remote Sensing in Ecology and Conservation, 8(4), 431-447.

Rimski-Korsakov, H., Alvarez, C. R., & Lavado, R. S. (2015). Cover crops in the agricultural systems of the Argentine Pampas. Journal of Soil and Water Conservation, 70(6), 134A-140A.

Robertson, G. P., Paul, E. A., & Harwood, R. R. (2000). Greenhouse gases in intensive agriculture: contributions of individual gases to the radiative forcing of the atmosphere. Science, 289(5486), 1922-1925.

Preprint not peer reviewed

This preprint research paper has not been peer reviewed. Electronic copy available at: https://ssrn.com/abstract=4661637

Rositano, F., Pessah, S., Durand, P., & Laterra, P. (2022). Coupled socio-ecological changes in response to soybean expansion along the 2001–2010 decade in Argentina. Anthropocene, 39, 100343.

Rockström, J., Steffen, W., Noone, K., Persson, Å., Chapin, F. S., Lambin, E. F., ... & Foley, J. A. (2009). A safe operating space for humanity. nature, 461(7263), 472-475.

Ruimy, A., Saugier, B., & Dedieu, G. (1994). Methodology for the estimation of terrestrial net primary production from remotely sensed data. Journal of Geophysical Research: Atmospheres, 99(D3), 5263-5283.

Running, S. W. (1990). Estimating terrestrial primary productivity by combining remote sensing and ecosystem simulation. In Remote sensing of biosphere functioning (pp. 65-86). New York, NY: Springer New York.

Sabajo, C. R., Le Maire, G., June, T., Meijide, A., Roupsard, O., & Knohl, A. (2017). Expansion of oil palm and other cash crops causes an increase of the land surface temperature in the Jambi province in Indonesia. Biogeosciences, 14(20), 4619-4635.

Schwaiger, H. P., and Bird, D. N. (2010). Integration of albedo effects caused by land use change into the climate balance: Should we still account in greenhouse gas units?. Forest Ecology and Management, 260(3), 278-286.

Segarra, J., Buchaillot, M. L., Araus, J. L., & Kefauver, S. C. (2020). Remote sensing for precision agriculture: Sentinel-2 improved features and applications. Agronomy, 10(5), 641.

Sieber, P., Ericsson, N., & Hansson, P. A. (2019). Climate impact of surface albedo change in Life Cycle Assessment: Implications of site and time dependence. Environmental Impact Assessment Review, 77, 191-200.

Staiano, L., Sans, G. H. C., Baldassini, P., Gallego, F., Texeira, M. A., & Paruelo, J. M. (2021). Putting the Ecosystem Services idea at work: Applications on impact assessment and territorial planning. Environmental Development, 38, 100570.

Sun, G., Caldwell, P., Noormets, A., McNulty, S. G., Cohen, E., Moore Myers, J., ... & Chen, J. (2011). Upscaling key ecosystem functions across the conterminous United States by a water-centric ecosystem model. Journal of Geophysical Research: Biogeosciences, 116(G3).

Teluguntla, P., Thenkabail, P. S., Oliphant, A., Xiong, J., Gumma, M. K., Congalton, R. G., ... & Huete, A. (2018). A 30-m landsat-derived cropland extent product of Australia and China using random forest machine learning algorithm on Google Earth Engine cloud

Preprint not peer reviewed

This preprint research paper has not been peer reviewed. Electronic copy available at: https://ssrn.com/abstract=4661637

computing platform. ISPRS journal of photogrammetry and remote sensing, 144, 325-340.

Tucker, C. J. (1979). Red and photographic infrared linear combinations for monitoring vegetation. Remote sensing of Environment, 8(2), 127-150.

Tucker, C. J., Justice, C. O., & Prince, S. D. (1986). Monitoring the grasslands of the Sahel 1984-1985. International Journal of Remote Sensing, 7(11), 1571-1581.

Valcarce-Diñeiro, R., Arias-Pérez, B., Lopez-Sanchez, J. M., & Sánchez, N. (2019). Multi-temporal dual-and quad-polarimetric synthetic aperture radar data for crop-type mapping. Remote Sensing, 11(13), 1518.

Van de Griend, A. A., and Owe, M. (1993). On the relationship between thermal emissivity and the normalized difference vegetation index for natural surfaces. International Journal of remote sensing, 14(6), 1119-1131.

Varela, M. F., Scianca, C. M., Taboada, M. A., & Rubio, G. (2014). Cover crop effects on soybean residue decomposition and P release in no-tillage systems of Argentina. Soil and Tillage Research, 143, 59-66.

Vega, E., Baldi, G., Jobbágy, E. G., & Paruelo, J. (2009). Land use change patterns in the Río de la Plata grasslands: the influence of phytogeographic and political boundaries. Agriculture, ecosystems & environment, 134(3-4), 287-292.

Verón, S. R., Blanco, L. J., Texeira, M. A., Irisarri, J. G. N., & Paruelo, J. M. (2018). Desertification and ecosystem services supply: The case of the Arid Chaco of South America. Journal of Arid Environments, 159, 66-74.

Viglizzo, E. F., Lértora, F., Pordomingo, A. J., Bernardos, J. N., Roberto, Z. E., & Del Valle, H. (2001). Ecological lessons and applications from one century of low external-input farming in the pampas of Argentina. Agriculture, ecosystems & environment, 83(1-2), 65-81.

Viglizzo, E. F., Frank, F. C., Carreño, L. V., Jobbagy, E. G., Pereyra, H., Clatt, J., ... & Ricard, M. F. (2011). Ecological and environmental footprint of 50 years of agricultural expansion in Argentina. Global change biology, 17(2), 959-973.

Viglizzo, E. F., Jobbágy, E. G., Ricard, M. F., & Paruelo, J. M. (2016). Partition of some key regulating services in terrestrial ecosystems: meta-analysis and review. Science of the Total Environment, 562, 47-60.

Viglizzo, E. F., Jobbágy, E. G., Carreño, L., Frank, F. C., Aragón, R., De Oro, L., & Salvador, V. (2009). The dynamics of cultivation and floods in arable lands of Central Argentina. Hydrology and Earth System Sciences, 13(4), 491-502.

Preprint not peer reviewed

This preprint research paper has not been peer reviewed. Electronic copy available at: https://ssrn.com/abstract=4661637

Virginia, R.A., Wall, D.H. 2001. Principles of ecosystem function. Encyclopedia of Biodiversity, 345-352

Vuolo, F., Neuwirth, M., Immitzer, M., Atzberger, C., & Ng, W. T. (2018). How much does multi-temporal Sentinel-2 data improve crop type classification?. International journal of applied earth observation and geoinformation, 72, 122-130.

Waldner, F., De Abelleyra, D., Verón, S. R., Zhang, M., Wu, B., Plotnikov, D., ... & Defourny, P. (2016). Towards a set of agrosystem-specific cropland mapping methods to address the global cropland diversity. International Journal of Remote Sensing, 37(14), 3196-3231.

Ward, D. S., and Mahowald, N. M. (2015). Local sources of global climate forcing from different categories of land use activities. Earth System Dynamics, 6(1), 175-194.

Ward, D. S., and Mahowald, N. M. (2014). Contributions of developed and developing countries to global climate forcing and surface temperature change. Environmental Research Letters, 9(7), 074008.

Wei, B., Bao, Y., Yu, S., Yin, S., & Zhang, Y. (2021). Analysis of land surface temperature variation based on MODIS data a case study of the agricultural pastural ecotone of northern China. International Journal of Applied Earth Observation and Geoinformation, 100, 102342.

Weyland, F., Baudry, J., & Ghersa, C. (2019). Short-term effects of a severe drought on avian diversity and abundance in a Pampas Agroecosystem. Austral Ecology, 44(8), 1340-1350.

Williams, C. A., Gu, H., & Jiao, T. (2021). Climate impacts of US forest loss span net warming to net cooling. Science Advances, 7(7), eaax8859.

8. Appendix

Calculation of spectral indices

We calculated four spectral indices based on Sentinel-2 reflectance data. The NDVI (Normalized Difference Vegetation Index) (Running 1990), was calculated as follows:

NDVI = (B8-B4) / (B8+B4)

where B8 and B4 correspond to the reflectance in the near infrared (842 nm) and red (665 nm) portion of the electromagnetic spectrum, respectively.

Preprint not peer reviewed

This preprint research paper has not been peer reviewed. Electronic copy available at: https://ssrn.com/abstract=4661637

The GNDVI (Green Normalized Difference Vegetation Index) (Gitelson et al. 1996), was calculated as follows:

GNDVI = (B8-B3) / (B8+B3)

where B8 and B3 correspond to the reflectance in the near infrared (842 nm) and green (560 nm) portion of the electromagnetic spectrum, respectively.

The NDMI (Normalized Difference Moisture Index) (Hardinsky et al. 1983), was calculated as follows:

NDMI = (B8-B11) / (B8+B11)

where B8 and B11 correspond to the reflectance in the near infrared (842 nm) and short-wave infrared (1375 nm) portion of the electromagnetic spectrum, respectively.

The NBRI (Normalized Burn Ratio Index) (Key and Benson 1999), was calculated as follows:

NBRI = (B8-B12) / (B8+B12)

where B8 and B12 correspond to the reflectance in the near infrared (842 nm) and short-wave infrared (1610 nm) portion of the electromagnetic spectrum, respectively.

Radiation Calculation

It was estimated from the net incident shortwave radiation Sn (Mj m^{-2} day^{-1}) and the net emitted longwave radiation Ln (Mj m^{-2} $day^{-1)}$ as proposed by Granger (2000):

(a) Rn = Sn + Ln

where Sn was estimated from the global shortwave radiation St (Mj m^{-2} day^{-1}) proposed by Shuttleworth (1993) and the albedo (α) according to Liang (2000).

(b) Sn = St (1 – α)

(c) Ln = -4.25 - 0.24 St

To estimate the shortwave radiation (Sn), we considered the estimation proposed by Shuttleworth (1993), where the total incident shortwave radiation (St) was calculated according to

(d) St = (a + b m M-1) So

This preprint research paper has not been peer reviewed. Electronic copy available at: https://ssrn.com/abstract=4661637

where the calculation considers the effective sunshine (m) and the total day length (M) in hours, a and b are constants that assume fixed values of 0.25 and 0.5 respectively for temperate climates. The extraterrestrial solar radiation So (mm dia^{-1}) was calculated as:

(e) $So = 15.392\, dr\, (\omega \sin\Phi \sin\delta + \cos\Phi \sin\omega)$

where dr is the relative distance between the earth and the sun, ω is the solar hour angle, δ is the solar declination and Φ is the latitude of the study area.

Preprint not peer reviewed

This preprint research paper has not been peer reviewed. Electronic copy available at: https://ssrn.com/abstract=4661637